BIOCHEMISTRY
including biophysical chemistry & molecular biology

Article

pubs.acs.org/biochemistry

Prechemistry Nucleotide Selection Checkpoints in the Reaction Pathway of DNA Polymerase I and Roles of Glu710 and Tyr766

Oya Bermek,† Nigel D. F. Grindley, and Catherine M. Joyce*

Department of Molecular Biophysics and Biochemistry, Yale University, New Haven, Connecticut 06520, United States

Supporting Information

ABSTRACT: The accuracy of high-fidelity DNA polymerases such as DNA polymerase I (Klenow fragment) is governed by conformational changes early in the reaction pathway that serve as fidelity checkpoints, identifying inappropriate template−nucleotide pairings. The fingers-closing transition (detected by a fluorescence resonance energy transfer-based assay) is the unique outcome of binding a correct incoming nucleotide, both complementary to the templating base and with a deoxyribose (rather than ribose) sugar structure. Complexes with mispaired dNTPs or complementary rNTPs are arrested at an earlier stage, corresponding to a partially closed fingers conformation, in which weak binding of DNA and nucleotide promote dissociation and resampling of the substrate pool. A 2-aminopurine fluorescence probe on the DNA template provides further information about the steps preceding fingers closing. A characteristic 2-aminopurine signal is observed on binding a complementary nucleotide, regardless of whether the sugar is deoxyribose or ribose. However, mispaired dNTPs show entirely different behavior. Thus, a fidelity checkpoint ahead of fingers closing is responsible for distinguishing complementary from noncomplementary nucleotides and routing them toward different outcomes. The E710A mutator polymerase has a defect in the early fidelity checkpoint such that some complementary dNTPs are treated as if they were mispaired. In the Y766A mutant, the early checkpoint functions normally, but some correctly paired dNTPs do not efficiently undergo fingers closing. Thus, both mutator alleles cause a blurring of the distinction between correct and incorrect base pairs and result in a larger fraction of errors passing through the prechemistry fidelity checkpoints.

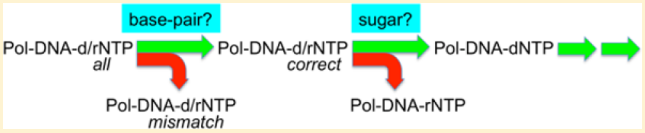

High-fidelity DNA polymerases, such as *Escherichia coli* DNA polymerase I (Klenow fragment) [Pol I(KF)], copy a DNA template with an accuracy far greater than would be expected on the basis of the energetics of base pairing.[1] This accuracy is attributed to a sequence of noncovalent steps, preceding the chemical step of phosphoryl transfer, which act as kinetic checkpoints ensuring that only a complementary nucleotide with a deoxyribose sugar progresses efficiently toward product formation.[2] During each synthetic cycle *in vivo*, the correct dNTP is outnumbered by three noncomplementary dNTPs and a 10−100-fold excess of the corresponding rNTP[3,4] but these are detected at the early checkpoints, resulting in their rejection before commitment to the chemistry step.

Cocrystal structures of *Bacillus stearothermophilus* DNA polymerase (*Bst* DNA pol), a very close A-family homologue of Pol I(KF), provide snapshots of important conformations likely to be part of the prechemistry steps in the reaction mechanism (Figure 1). The open Pol−DNA binary complex (panel A) and the closed Pol−DNA−dNTP ternary complex (panel C), formed in the presence of a complementary dNTP (under conditions where the chemical step of incorporation cannot take place), have been observed in many high-fidelity DNA polymerases.[5−10] The open and closed conformations differ by a substantial movement of a segment of the fingers subdomain, including helix O that contains several important active-site residues. More recently, partially closed ternary complexes have been observed with *Bst* DNA pol in the presence of a mismatched dNTP or a complementary rNTP;[11,12] in these structures, the mobile part of the fingers subdomain appears to be on the trajectory between the open and closed conformations, suggesting that the partially closed conformation might be an important intermediate in the prechemistry steps.

Our single-molecule FRET (smFRET) studies of Pol I(KF) also indicate the existence of a conformation intermediate between open and closed complexes.[13,14] The position of the fingers subdomain was reported using FRET between a donor fluorophore on the mobile portion of the fingers subdomain and an acceptor on the thumb subdomain (green and red spheres, respectively, in Figure 1). As expected, the binary complex had the majority of polymerase molecules in the open conformation and the ternary complex with a complementary dNTP had the majority in the fingers-closed conformation. In the presence of mispaired dNTPs or complementary rNTPs, a novel intermediate-FRET species was abundant in the molecular population. Moreover, the FRET value of this species was consistent with the probe positions predicted from the cocrystal structure of the *Bst* DNA pol partially closed mispaired ternary complex. Thus, it appears that an intermediate conformation accumulates when the DNA polymerase binary complex binds an inappropriate nucleotide

Received: June 27, 2013
Revised: August 7, 2013
Published: August 12, 2013

   dx.doi.org/10.1021/bi400837k | *Biochemistry* 2013, 52, 6258−6274

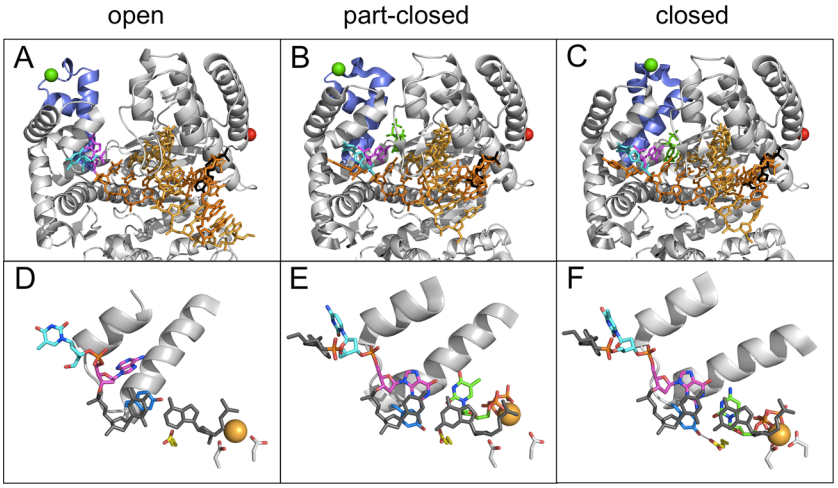

Figure 1. Conformations of A-family DNA polymerases illustrated using structural data from *Bst* DNA pol. In panels A−C, the protein backbone is colored gray, except for the portion of the fingers subdomain from residue 680 to 714 [equivalent to residues 732−766 in Pol I(KF)] whose position changes during the fingers-closing transition (blue). The green and red spheres mark the positions of residues 692 and 498, respectively, equivalent to residues 744 and 550 in Pol I(KF), respectively, used for attachment of fluorescent probes in this study and others. The duplex DNA substrate is colored orange, with the template strand darker than the primer strand. The templating base, T(0), is colored magenta, and its 5′ neighbor, T(+1), is colored cyan. The T(−8) position, the location of a dabcyl quencher in the FRET-based assay for fingers closing, is colored black. The incoming dNTP, where present, is shown in stick representation in green. Panels D−F show an expanded view of the polymerase active-site region. Helices O and O_1 of the protein are illustrated as ribbons. The T(0) and T(+1) bases and the incoming dNTP are colored as in panels A−C; the primer-terminal base pair is colored dark gray. Each structure has a single divalent metal ion at the active site, represented by a gold sphere. The E658 and Y714 side chains (equivalent to residues E710 and Y766, mutated in our study) are colored blue and yellow, respectively. The two carboxylate ligands to the catalytic metal ions are colored pale gray; from left to right, they are D830 and D653 [D882 and D705, respectively, in Pol I(KF)]. This figure was made using PyMOL (Schrödinger, LLC). The coordinate files used are the open conformation from PDB entry 4BDP (A and D),[38] the partially closed conformation, with mispaired G-dTTP, from PDB entry 3HP6 (B and E),[11] and the closed conformation, with correctly paired G-dCTP, from PDB entry 2HVI (C and F).[39]

substrate, raising the possibility that this complex may be involved in the kinetic steps that serve as checkpoints for correct substrate selection. A more recent smFRET study of Pol I(KF), using probes on the protein and DNA, is also consistent with this model.[15]

In our lab, we have developed two different ensemble fluorescence assays to investigate prechemistry conformational transitions in Pol I(KF).[16−18] One reports the fingers-closing transformation using a donor fluorophore on the fingers subdomain, as in the smFRET study (green sphere in Figure 1), and a quencher located on the DNA template strand, eight bases back from the terminal base pair (black in Figure 1). The other uses a fluorescent DNA base analogue, 2-aminopurine (2-AP), that reports changes to the environment of the T(+1) base, 5′ to the templating base (cyan in Figure 1). In this study, we have used these two assays to characterize the conformational shifts associated with all four correctly paired ternary complexes, all 12 mispairs, and several rNTP-containing complexes. In WT Pol I(KF), we show that the closed complex is highly populated only in the presence of a complementary nascent base pair, while all other ternary complexes fail to progress efficiently beyond the (presumed) partially closed state. The T(+1)2-AP reporter distinguishes a variety of species within the family of partially closed complexes, indicating that different types of ternary complexes reach distinct conformational end points.

In Pol I(KF), two active-site side chains, E710 and Y766, play important roles in maintaining selectivity in the polymerase reaction, as shown by the reduced fidelity (mutator phenotype) associated with some mutations in these residues.[19−23] Together, these two side chains define the boundaries of the pocket that binds and constrains the shape of the nascent base pair (Figure 1D−F): Y766 (blue) on the template side and E710 (yellow) on the dNTP side. In the transitions illustrated in Figure 1D−F, Y766 moves to create space in the binding pocket for the templating base. The contact surface between E710 and the nucleotide contributes to nucleotide binding affinity as well as providing steric constraints that hinder formation of a fully closed conformation with complementary ribonucleotides.[24] In cocrystals of fully closed ternary complexes, the homologues of Y766 and E710 are linked via a hydrogen bond (Figure 1F). Here we use substitutions at Y766 and E710 to investigate the role of these side chains in the prechemistry fidelity checkpoints.

EXPERIMENTAL PROCEDURES

Materials. DNA oligonucleotides for fluorescence and kinetics experiments were synthesized by the Keck Biotechnology Resource Laboratory at Yale Medical School and purified by denaturing gel electrophoresis. Ultrapure deoxynucleotides and [γ-^{32}P]ATP were purchased from Amersham Pharmacia Biosciences (GE Healthcare).

Expression, Purification, and IAEDANS Labeling of Pol I(KF). Expression and purification of the Pol I(KF) construct used for fluorophore labeling have been described previously.[17,25] The protein has an N-terminal hexahistidine tag for nickel chelate affinity purification, the D424A mutation to inactivate the 3′−5′ exonuclease, the C907S mutation to remove the single native cysteine, and the L744C mutation to provide a unique labeling site on the fingers subdomain. These changes have no significant effect on DNA polymerase activity.[17] The N-His_6/D424A/C907S/L744C protein, termed the wild type (WT), was labeled with IAEDANS (Molecular Probes, Eugene, OR) as described previously.[18] The E710A,

dx.doi.org/10.1021/bi400837k | *Biochemistry* 2013, 52, 6258−6274

E710Q, Y766A, and Y766F mutations were introduced into the Pol I(KF) construct described above, using the QuikChange site-directed mutagenesis kit (Stratagene), according to the manufacturer's instructions.

Chemical Quench Experiments. Single-turnover measurements of nucleotide incorporation were made at room temperature (22 °C) in a rapid quench-flow instrument (KinTek Corp. model RQF-3). The DNA substrate was the linear duplex L:unmod:3′OH (Figure 2A), consisting of a 13-mer primer, 5′-labeled with ^{32}P (or, in a few experiments, Cy5), annealed to a 1.5-fold molar excess of the complementary 19-mer, with A, C, G, or T as the templating base. The reaction was initiated by rapid mixing of an enzyme/DNA solution (typically 2 μM polymerase and 0.2 μM primer–template duplex) with an equal volume of a dNTP solution. Our standard polymerase reaction buffer, used in all experiments, consisted of 50 mM Tris-HCl (pH 7.5), 1 mM EDTA, and 10 mM $MgCl_2$. Reactions were quenched at appropriate time intervals with excess EDTA, and mixtures were fractionated on denaturing polyacrylamide–urea gels and quantitated on a Fuji FLA 5100 scanner.

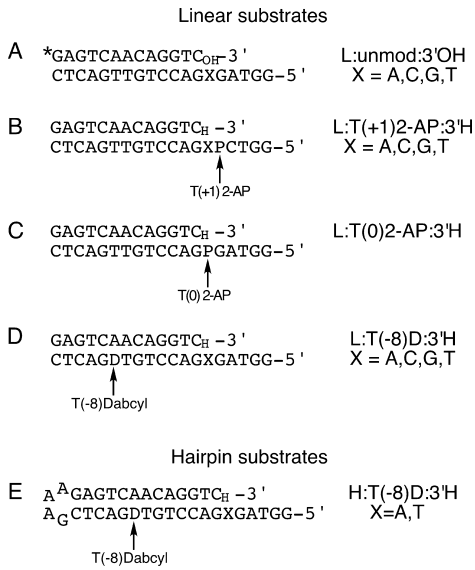

Figure 2. DNA oligonucleotides used in this study. (A) DNA substrate used in chemical quench experiments. The 13-mer primer, 5′-labeled (indicated with an asterisk) with either ^{32}P or Cy5, was annealed to the 19-mer template. (B) DNA duplex oligonucleotide used for 2-AP fluorescence measurements. The 2-AP fluorophore (P) is 5′ to the templating base, designated as the T(+1) position. (C) DNA duplex oligonucleotide having 2-AP at the templating, T(0), position. (D) DNA substrate used in FRET-based fluorescence measurements of fingers closing. The dabcyl-dT quencher (D) was placed at the T(−8) position. (E) Similar to D, but a hairpin DNA duplex, used in FRET-based assays of fingers closing. Except for panel A, the primer strand was dideoxy-terminated (3′H) to prevent the reaction from proceeding beyond the ternary complex. To avoid having a run of three consecutive G residues, the 5′ end of the template strand had the sequence 5′GGTATG when the templating base (underlined) was G.

Incorporation of mismatched dNTPs (at a final concentration of 1 mM) was measured using the same approach, but with manual sampling because of the slower reaction rate. To remove any traces of the dNTP complementary to the template base, a 2 mM solution of the dNTP was pretreated for 5 min at 22 °C with 1.1 μM Pol I(KF) and 0.4 μM unlabeled duplex with the same template base that was to be used in the incorporation experiment. This dNTP solution, now depleted of impurities of the dNTP complementary to the templating base, was then added to the mixture of polymerase and labeled DNA, as described above.

Fluorescence Emission Spectra. Steady-state fluorescence spectra of 2-AP were recorded at 22 °C using a Photon Technology International scanning spectrofluorometer. Solutions contained 1 μM L:T(+1)2-AP:3′H duplex DNA (Figure 2B), formed by annealing the T(+1)2-AP template strand with a 1.5-fold molar excess of the complementary primer strand, and 2 μM Pol I(KF) in polymerase reaction buffer. Nucleotides were added to a final concentration of 1 mM. Samples were excited at 310 nm, and emission spectra were scanned from 330 to 460 nm. Spectra were corrected by subtraction of the fluorescence emission contributed by the identical concentration of Pol I(KF), with nucleotides where appropriate.

Stopped-Flow Fluorescence. Stopped-flow experiments were performed at 22 °C using an Applied Photophysics SX.18MV spectrofluorometer. For measurements using the T(+1)2-AP reporter, one drive syringe contained a solution of L:T(+1)2-AP:3′H duplex DNA with Pol I(KF) and the other contained nucleotide (complementary or mismatched dNTP, or rNTP), all in polymerase reaction buffer. Rapid mixing of the two solutions gave final concentrations of 0.5 μM DNA and 1 μM Pol I(KF), with varied nucleotide concentrations (indicated in the figures). The excitation wavelength for the 2-AP probe was 313 nm, and fluorescence emission was detected using a 345 nm long-pass filter.

For FRET-based stopped-flow experiments reporting the fingers-closing transition, one drive syringe contained AEDANS-labeled Pol I(KF) and the dabcyl-modified H:T(−8)D:3′H or L:T(−8)D:3′H DNA (Figure 2) while the other contained the nucleotide. The final concentrations after mixing were 0.5 μM labeled Pol I(KF) and 1 μM DNA. The excitation wavelength for the AEDANS reporter was 350 nm, and fluorescence emission was detected with a 400 nm long-pass filter.

DNA dissociation rates were measured by stopped-flow methods using either of these reporters. One drive syringe contained either 0.1 μM L:T(+1)2-AP:3′H duplex DNA and 0.2 μM Pol I(KF) (2-AP probe) or 0.1 μM AEDANS-labeled Pol I(KF) and 0.2 μM H:T(−8)D:3′H DNA (FRET assay). The second drive syringe contained an unmodified DNA duplex (2 μM). When the two solutions are mixed, the large excess of unmodified DNA acts as a trap, preventing the modified DNA molecules from rebinding to the polymerase, and the resulting fluorescence change reports DNA dissociation. To measure the dissociation of DNA from Pol–DNA–dNTP ternary complexes, the DNA trap solution also contained 2 mM dNTP.

In a typical stopped-flow experiment, data were collected for 10 s using a logarithmic time base, and averages were taken from four or more traces. Reaction rate constants were derived from curve fitting to exponential equations using Kaleidagraph (Synergy Software, Reading, PA).

In many of our stopped-flow experiments, we needed to compare the signal levels for several different nucleotides, all at the same instrument settings. Over the course of a long series of measurements, changes in lamp intensity could be misinterpreted as fluorescence changes; this problem was particularly acute for the FRET-based experiments because the overall signal changes tended to be smaller than with the 2-AP

dx.doi.org/10.1021/bi400837k | *Biochemistry* 2013, 52, 6258–6274

probe. Under such circumstances, we conducted multiple measurements of the buffer-only control (binary complex) throughout the experiment. Typically, the lamp intensity decreased as the experiment proceeded; to assess whether a particular nucleotide addition caused a FRET change, its stopped-flow trace was compared with buffer-only traces taken around the same time.

RESULTS

To report the rates of different steps within the Pol I(KF) reaction pathway, we used the DNA substrates shown in Figure 2. The duplex with an extendable (3′OH) primer terminus (A) was used in chemical quench experiments, providing information about the entire reaction up to and including covalent incorporation of the nucleotide. The DNAs used in fluorescence experiments (B–E) had nonextendable (dideoxy: 3′H) primers to focus on prechemistry intermediates. To investigate the roles of active-site side chains E710 and Y766, we introduced mutations into a Pol I(KF) construct that also had the L744C mutation for fluorophore labeling of the protein. At both positions, we studied the alanine replacement and also the more conservative E710Q and Y766F mutations.

Correct and Incorrect Nucleotide Incorporation Kinetics. Using four DNA duplexes with essentially the same sequence except for the templating bases (Figure 2A), we measured the rate of incorporation of each correctly paired dNTP by WT Pol I(KF) under single-turnover conditions. The pre-steady-state kinetic constants, k_{pol} and K_d, obtained from plots of the rate constants (k_{obs}) as a function of dNTP concentration (Figure S1 of the Supporting Information), show significant variation in the kinetics of incorporation of the four complementary base pairs (Table 1). Especially noteworthy are the faster rate for dATP incorporation and the substantially tighter binding of dGTP in this particular sequence context.

For the mutant proteins, single-turnover measurements of the incorporation of dTTP opposite a template A showed that the E710A, E710Q, and Y766A mutations caused substantial decreases in the reaction rate and dTTP binding affinity, whereas Y766F was very similar to WT except for ∼2-fold weaker binding of dTTP (Table 1). The effect of the Y766A mutation on incorporation kinetics was base pair-specific; the k_{pol} and K_d parameters were each ∼10-fold less favorable than those of WT for A-dTTP incorporation, but very similar to those of WT for G-dCTP incorporation. Rates for C-dGTP and T-dATP incorporation were intermediate between these two extremes (data not shown).

Misinsertion rates for WT Pol I(KF), measured using the same four DNA duplexes and 1 mM mismatched dNTPs, varied over nearly 2 orders of magnitude (Table 2 and Figure S2A,B of the Supporting Information). The fastest misincorporations (T-dGTP and C-dATP) were ∼500-fold slower than incorporation of correctly paired dNTPs, and the slowest (C-dCTP and A-dGTP) were ∼50000-fold slower. Because a complementary dNTP is incorporated much more efficiently than a mismatch, misinsertion kinetic measurements can be compromised if the mismatched dNTP is contaminated with even a small fraction of a complementary dNTP. An obvious example is the presence of dUTP as a contaminant formed by deamination of dCTP, but we have observed other instances in which a dNTP contains a low-level contaminant with a different coding potential. To eliminate this problem, we devised a simple procedure for removing such contaminants: the dNTP was first exposed to Pol I(KF) and the unlabeled DNA, to remove any complementary dNTP by incorporation, before addition of the corresponding labeled DNA to measure the kinetics of misinsertion (see Experimental Procedures and Figure S2C,D of the Supporting Information).

The DNA Rearrangement of Step 2.1 Reveals Multiple Steps with Complementary dNTPs. A 2-AP fluorescent probe 5′ to the templating base [the T(+1) position (Figure 2B)] reports the early prechemistry step 2.1 that precedes fingers closing.[16,18] With WT Pol I(KF) and a nonextendable DNA, this step is detected in the stopped-flow instrument as a rapid fluorescence increase, attributed to unstacking of the T(+1)2-AP from its immediate neighbors,[26] whose rate and amplitude are dependent on the concentration of the complementary dNTP (Figure 3A). Figure 4 (left-most column) shows data for all four template bases and, in each

Table 1. Single-Turnover Kinetic Data for the Incorporation of Complementary dNTPs[a]

Pol I(KF)[b]	base pair	$K_{d(dNTP)}$ (μM)	k_{pol} (s^{-1})	k_{pol}/K_d (M^{-1} s^{-1})
WT	C-dGTP	2.9 ± 0.1	46 ± 1	1.6×10^7
WT	G-dCTP	9.4 ± 0.5	63 ± 5	6.7×10^6
WT	T-dATP	8.6 ± 0.7	110 ± 2	1.2×10^7
WT	A-dTTP	17 ± 1	40 ± 2	2.3×10^6
E710A	A-dTTP	110 ± 10	0.26 ± 0.01	2.4×10^3
E710Q	A-dTTP	320 ± 20	0.23 ± 0.01	7.2×10^2
Y766A	A-dTTP	150 ± 40	5.0 ± 0.6	3.3×10^4
Y766F	A-dTTP	41 ± 4	50 ± 3	1.2×10^6
WT	G-dCTP[c]	6.7	30	4.5×10^6
Y766A	G-dCTP[c]	8.2	25	3.0×10^6

[a]Using the duplex DNA substrates listed in Figure 2A. Data reported as means ± the standard error are average values from at least two experiments; the others are single measurements. The data for WT Pol I(KF) are in good agreement with previous measurements.[17] [b]All the proteins had the genotype N-His_6/D424A/L744C/C907S in addition to the listed mutations. [c]These measurements were taken using a 5′-Cy5-labeled substrate, which gives an ∼2-fold lower k_{pol} compared with that of the corresponding ^{32}P-labeled DNA. All the other rate measurements were taken using 5′-^{32}P-labeled DNA.

Table 2. Rate Constants for Misinsertion by WT Pol I(KF)[a]

base pair	k_{obs} (s^{-1}) at 1 mM dNTP
A-dATP	0.054 ± 0.004
A-dCTP	0.013 ± 0.001
A-dGTP	0.0016 ± 0.0001
C-dATP	0.086 ± 0.009
C-dCTP	0.0014 ± 0.0001
C-dTTP	0.0041 ± 0.0005
G-dATP	0.057 ± 0.005
G-dGTP	0.036 ± 0.005
G-dTTP	0.049 ± 0.003
T-dCTP	0.028 ± 0.003
T-dGTP	0.098 ± 0.001
T-dTTP	0.012 ± 0.001

[a]Using the duplex DNA substrates listed in Figure 2A. Rate constants for dNTP misinsertion in the presence of 1 mM dNTP were measured in duplicate and are reported as means ± the standard deviation. See Figure S2 of the Supporting Information for examples of misinsertion time courses.

dx.doi.org/10.1021/bi400837k | Biochemistry 2013, 52, 6258–6274

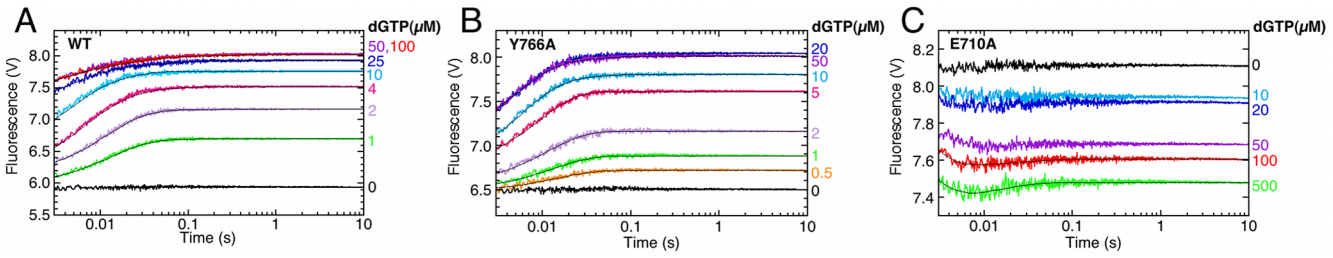

Figure 3. Stopped-flow fluorescence experiments using DNA duplexes with the T(+1)2-AP reporter (Figure 2B). The fluorescence traces were observed upon addition of dGTP, at the indicated concentrations, opposite a template C for WT (A), Y766A (B), and E710A (C). Time is plotted on a logarithmic scale to display clearly all phases of the reaction. The black lines superimposed on the data traces show fitting to double- or triple-exponential equations, giving the parameters reported in Table S1 of the Supporting Information (see Figure S3 of the Supporting Information for examples of curve fitting and residuals).

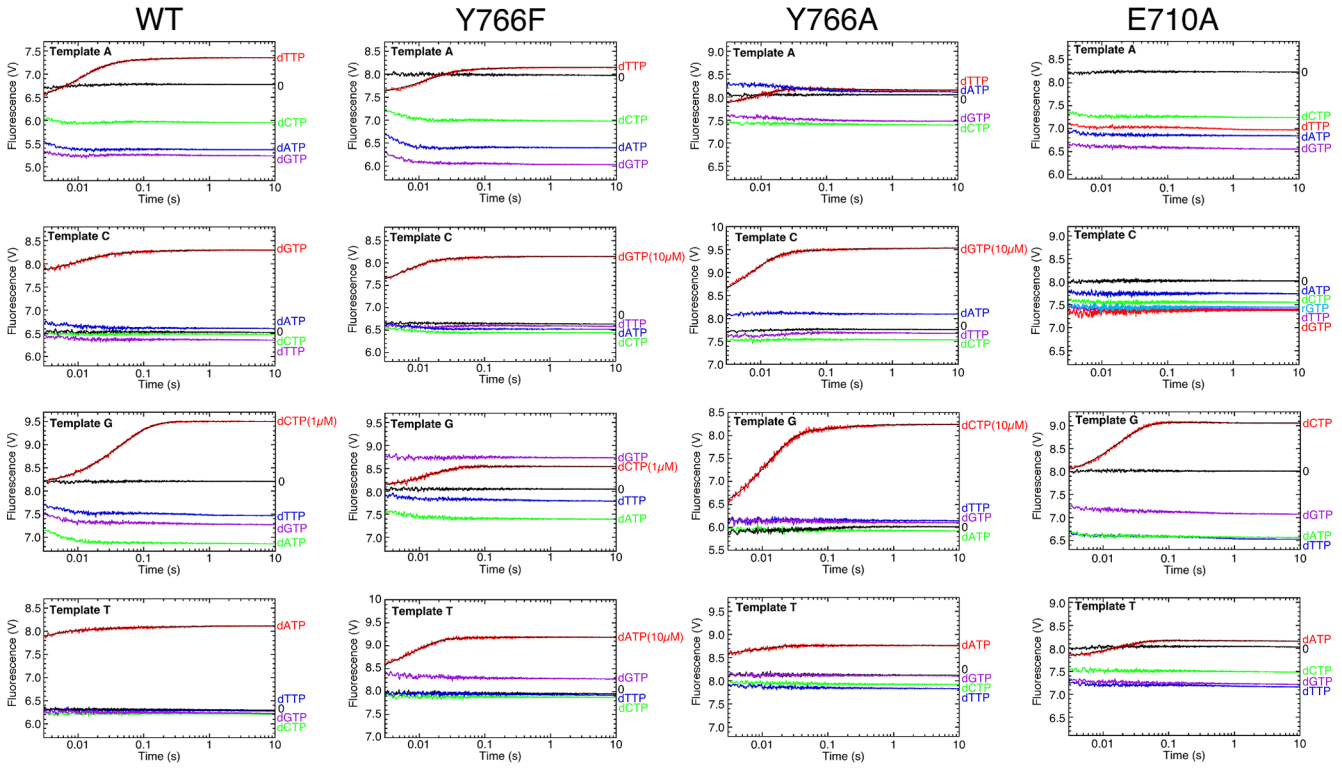

Figure 4. Ternary complex formation, by WT, Y766F, Y766A, and E710A Pol I(KF), at all four template bases examined by stopped-flow fluorescence using the T(+1)2-AP reporter. The traces show the fluorescence signal upon addition of correct or mismatched nucleotides to a binary complex of Pol I(KF) with each 2-AP-containing DNA duplex (Figure 2B). For each panel, the PMT voltage was set at a level appropriate for the range of that particular experiment and maintained at this setting throughout, allowing comparison of the fluorescence signals resulting from each nucleotide. All nucleotides were at a final concentration of 1 mM unless a lower concentration is indicated. (For template G, Figure S4H of the Supporting Information shows the traces observed at high dCTP concentrations, with a substantial fluorescence increase in the instrument dead time.) The traces marked 0 correspond to addition of reaction buffer, showing the fluorescence of the binary complex. The black lines superimposed on some data traces show fitting to exponential equations, giving the parameters reported in Table S1 of the Supporting Information.

case, the complementary dNTP (red trace) elicits the characteristic fluorescence increase.

The fitting of these fluorescence traces to exponential equations to extract rate constants is not a simple process. Most of the traces fit best to a triple exponential (see Figure S3 of the Supporting Information for an example of curve fitting and residuals) but, for some, a double exponential is satisfactory. Our interpretation is that three processes contribute to the rate of the observed fluorescence change but that some of these processes are less apparent at the extremes of the concentration range; specifically, the slowest phase becomes insignificant at the lowest concentrations, whereas the fastest phase tends to be lost in the instrument dead time at the highest concentrations. At all but the lowest concentrations, the sum of the amplitudes from empirical triple (or double)-exponential fits fails to account for the entire observed fluorescence change relative to the buffer control (see WT data in Table 3). In a previous study,[18] we had assumed that the "missing amplitude" was part of the fastest of the fitted rates, and therefore, we constrained the exponential fits of our data to include the entire fluorescence change. The current study shows this assumption to be incorrect. When using a DNA duplex with a template A (Figure 4), the fluorescence change observed upon addition of the complementary dTTP originates at a point lower than the signal of the Pol–DNA binary complex (buffer-only control). Therefore, there must be an additional intermediate, with a

dx.doi.org/10.1021/bi400837k | *Biochemistry* 2013, 52, 6258–6274

Table 3. Kinetic Parameters of Wild-Type and Mutant Pol I(KF) in Stopped-Flow Fluorescence Experiments with a T(+1)2-AP Reporter

protein	reaction[a]	k_1 (s^{-1})	k_2 (s^{-1})	k_3 (s^{-1})	missing amplitude[b] (% of total)	$K_{d(overall)}$ (μM)[c]
WT[c]	A-dTTP (1 mM)	95 ± 9	21 ± 3	3.5 ± 0.3	−(58 ± 13)	
	C-dGTP (100 μM)	260	45	5.8	74	1.5
	C-dGTP (1 mM)	120	34	3.8	69	
	C-rGTP (1 mM)	94			79	41
	G-dCTP (100 μM)	130 ± 30	16 ± 3	1.5 ± 1.0	73 ± 6	0.60 ± 0.21
	T-dATP (100 μM)	230	27	2.1	80	
	T-dATP (1 mM)	380 ± 50	38 ± 7	2.2 ± 0.2	73 ± 3	
Y766F	A-dTTP (1 mM)	73 ± 3	7.1 ± 0.6			
	C-dGTP (1 mM)	110 ± 1	11 ± 1			5.9 ± 2.4
	C-rGTP (1 mM)	≥500[d]				68
	G-dCTP (1 μM)	68				
	T-dATP (1 mM)	≥500[d]				
Y766A	A-dTTP (1 mM)	120 ± 20	4.9 ± 1.5			
	C-dGTP (1 mM)	160 ± 20	28 ± 10			2.9 ± 2.0
	C-rGTP (1 mM)	180 ± 20	73 ± 34			13
	G-dCTP (1 mM)	220	12	0.67		
	T-dATP (1 mM)	110 ± 10				
E710A[e]	A-dTTP	like mispair				
	C-dGTP	like mispair				46 ± 13
	C-rGTP	like mispair				
	G-dCTP (1 mM)	58 ± 1				
	T-dATP (1 mM)	53 ± 9	0.52 ± 0.40			
E710Q	C-dGTP (1 mM)	44 ± 5				10 ± 1

[a]The sequences of DNA duplexes with 2-AP at the T(+1) position and all four possible templating bases are shown in Figure 2B. Concentrations of the complementary nucleotide are given in parentheses. Data reported as means ± the standard deviation are average values from two or more experiments; the others are from single determinations. The results for WT Pol I(KF) with C-dGTP are in good agreement with our previous work.[18] See Table S1 of the Supporting Information for a full list of rate constants and amplitudes relevant to the data in this table and Figure S3 of the Supporting Information for examples of curve fitting and residuals. [b]The total fluorescence change in going from the binary complex to the ternary complex was calculated by subtracting the start point of the buffer-only trace from the end point of the trace observed upon addition of the indicated concentration of the complementary dNTP. The sum of the fitted amplitudes (e.g., A1 + A2 + A3 for a triple exponential) was subtracted from the total fluorescence change to give the missing amplitude, for which the fitted data do not account. This is expressed as a percentage of the total fluorescence change. The value for the A-dTTP base pair is negative, indicating that the traces observed upon addition of dTTP started below the buffer-only (binary complex) signal. [c]$K_{d(overall)}$ was determined from titration experiments by plotting the end point of each fluorescence trace vs nucleotide concentration and fitting to a hyperbolic equation (Figure S4 of the Supporting Information). [d]Corresponds to a fluorescence increase that is ≥80% complete within the first 3 ms of data collection. [e]At templates A and C, the 2-AP fluorescence signal obtained with E710A upon addition of the complementary dNTP shows a decrease, as observed typically with mispairs (Figure 4).

distinct T(+1)2-AP fluorescence signal, that is formed within the first ∼1 ms and then undergoes further transformations resulting in the fluorescence trace recorded after the instrument dead time. At a template A, this intermediate has a 2-AP fluorescence signal lower than that of the binary complex. Assuming analogous intermediates are formed at templates C, G, and T, their fluorescence signals are almost certainly higher than those of the corresponding binary complexes. Emission spectra of WT binary and ternary complexes (Figure 5A) confirm the template-dependent differences seen in the stopped-flow traces and suggest that variability in the fluorescence of the binary complex (particularly the much higher fluorescence in the template A complex) is a major contributor to the observed templating base effects. Because the existence of an additional intermediate creates uncertainty with regard to the start point of the T(+1)2-AP fluorescence traces, reaction rates were calculated from empirical exponential fits of the observable portion of the fluorescence change, without further adjustment.

The rates of the 2-AP fluorescence change were similar for all four correct base pairs with WT Pol I(KF) (Table 3): a rapid first phase of ∼100−300 s^{-1} and a slower second phase of ∼20−50 s^{-1}. In some cases, the fit was slightly improved by including a low-amplitude final phase of ∼1−5 s^{-1}. At high dNTP concentrations, more than half of the total fluorescence change goes unrecorded in the first few milliseconds (missing amplitude in Table 3); of the remaining amplitude, the first phase typically accounts for ≥70%, the second phase ∼20%, and the third phase ≤10% (Table S1 of the Supporting Information). A complementary ribonucleotide (C-rGTP) elicited a fluorescence change whose early stages resemble that of the corresponding dNTP (Figure 6A): a substantial fluorescence increase in the instrument dead time followed by an increase at a rate of ∼100 s^{-1}. However, the overall amplitude was lower; there were no detectable changes corresponding to the second and third phases observed with dNTPs, and the dissociation constant [$K_{d(overall)}$], measured from the end points of the fluorescence traces (Figure S4 of the

dx.doi.org/10.1021/bi400837k | Biochemistry 2013, 52, 6258−6274

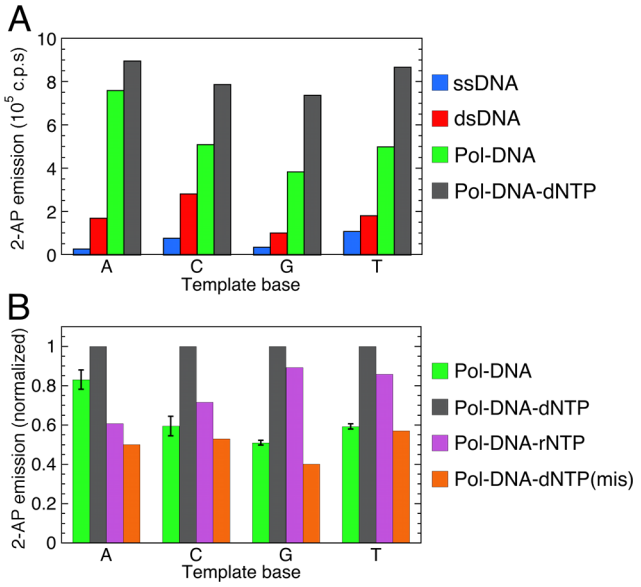

Figure 5. Fluorescence emission spectra of T(+1)2-AP DNAs with all four template bases (Figure 2B). The bars indicate the fluorescence signal at the 2-AP emission maximum after appropriate corrections (see Experimental Procedures). (A) Fluorescence of each 2-AP template strand oligonucleotide alone (blue), annealed to its complementary primer (red), as a binary complex with Pol I(KF) (green), and as a ternary complex with the complementary incoming dNTP (gray). (B) To aid comparison among the four template bases, the fluorescence signals for each templating base were normalized relative to the corresponding complementary dNTP ternary complex (gray). The Pol–DNA binary complex (green), the ternary complex with a complementary ribonucleotide (purple), and ternary mismatch complexes A-dGTP, C-dTTP, G-dATP, and T-dCTP (orange) were examined. Error bars on the binary complex data indicate the reproducibility of three independent measurements.

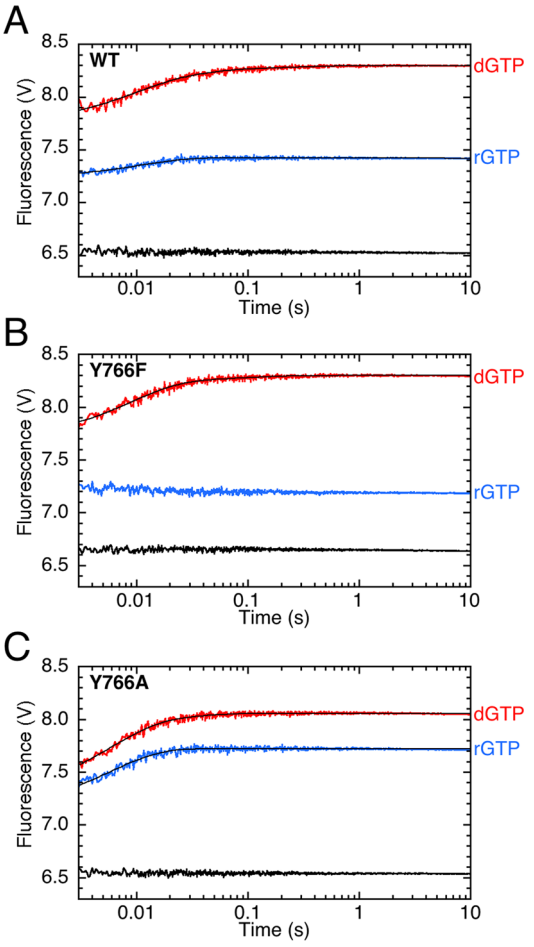

Figure 6. Ternary complex formation with a complementary rNTP examined by stopped-flow fluorescence using the T(+1)2-AP reporter (Figure 2B). The fluorescence change resulting from addition of rGTP (final concentration of 1 mM) to a Pol–DNA binary complex with a template C is compared with that observed with the same concentration of dGTP, for WT (A), Y766F (B), and Y766A (C). The black lines superimposed on some data traces show fitting to exponential equations, giving the parameters reported in Table S1 of the Supporting Information. The lack of a subsequent efficient fingers-closing step with the rNTP complex results in lower amplitudes for the T(+1)2-AP fluorescence changes [and also lower equilibrium fluorescence of complementary rNTP complexes relative to that of dNTP complexes (Figure 5B)] because the equilibrium will not be displaced as effectively in the direction of products.

Supporting Information), was ~30-fold higher for rGTP than for dGTP (Table 3).

A Different Active-Site Rearrangement Is Detected by the T(+1)2-AP Probe with Mispaired dNTPs. In contrast to the addition of complementary dNTPs, the addition of mispaired dNTPs to a WT Pol–DNA binary complex results in either very little fluorescence change or a fluorescence decrease (Figures 4 and 5B). In a stopped-flow experiment, the majority of mispairs showed a fast (~200–500 s^{-1}), low-amplitude fluorescence decrease; this rate is too fast to be explained by DNA dissociation, which would likewise result in a fluorescence decrease (see below). The fluorescence changes, relative to the binary complex start point, were more pronounced at template purines and were larger for purine–purine mispairs than for purine–pyrimidine mispairs. The mispair results indicate that the step 2.1 DNA rearrangement observed with a complementary dNTP or rNTP does not occur if the incoming nucleotide forms a mispair with the templating base; instead, mispairs may follow a different pathway or group of related pathways.

A T(0)2-AP Probe Also Distinguishes Complementary Nucleotides from Mispaired Nucleotides. In agreement with previous results,[16] a 2-AP probe at the templating base [T(0) (Figure 2C)] reports an early rapid step, much of which occurs within the dead time of the stopped-flow instrument, on binding the complementary dTTP (Figure 7). The fluorescence decrease associated with this step is believed to result from an increased level of stacking of the nascent base pair onto the primer terminal base pair as the incoming nucleotide engages with the templating base. The reaction rate mirrors our observations with the T(+1)2-AP probe: an initial very fast rate followed by a process at a rate similar to the T(+1) probe $Rate_1$. Addition of mispaired dNTPs or the complementary rUTP gave a much smaller fluorescence decrease, suggesting that they fail to engage effectively with the 2-AP template and do not progress as far along the reaction pathway as the complementary dTTP.

Y766 Is Not Required for Step 2.1. Using the T(+1)2-AP probe to report step 2.1, the fluorescence traces for Y766F and Y766A showed the characteristic fluorescence increase with all four correct base pairs (red traces in Figure 4). Moreover, the change in signal relative to that of the binary complex (black traces) was similar to that observed for WT, even including the decrease in the dead time seen with the A-dTTP pair. The

dx.doi.org/10.1021/bi400837k | *Biochemistry* 2013, 52, 6258–6274

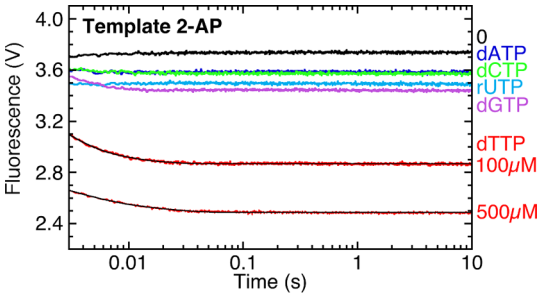

Figure 7. Ternary complex formation at a 2-AP templating base, monitored by stopped-flow fluorescence using the 2-AP signal. The traces show the fluorescence signal upon addition of complementary or mismatched dNTPs, or a complementary rNTP, to a binary complex of Pol I(KF) with the DNA duplex shown in Figure 2C. Except for the complementary dTTP, whose final concentrations are indicated, the other nucleotides were added to a final concentration of 500 μM. The black lines superimposed on the dTTP traces show fitting to a double-exponential equation, giving the parameters reported in Table S1 of the Supporting Information. For 100 μM dTTP, data from three independent experiments gave a k_1 of 490 ± 100 s^{-1} and a k_2 of 84 ± 33 s^{-1}.

$K_{d(overall)}$ values for the prechemistry steps, obtained by measuring the fluorescence end point as a function of dGTP concentration (Figure 3 and Figure S4 of the Supporting Information), were within ~4-fold for WT, Y766F, and Y766A, with Y766F showing the weakest dNTP binding (Table 3). For both mutants, the rates of the 2-AP fluorescence changes were similar to that of WT (Table 3); moreover, Y766A did not show the base pair-specific differences seen in its correct dNTP incorporation rates.

The Y766 mutants showed some small differences from WT Pol I(KF) in the 2-AP fluorescence changes when binding a complementary rNTP (Figure 6). The size of the fluorescence increase was always less for rNTP than for dNTP, but the difference was greatest for Y766F and smallest for Y766A, with WT in between. The "$Rate_1$" portion of the rNTP fluorescence traces (following the initial dead time fluorescence increase) had a larger amplitude for Y766A than for WT. By contrast, the $Rate_1$ fluorescence increase was absent in the Y766F trace, suggesting that the corresponding conformational transition is either too fast to detect or completely absent. The discrimination against rNTPs in the prechemistry steps, reflected in the $K_{d(overall)}$ values for dGTP and rGTP, is ~25-fold for WT and at least 2-fold lower for the Y766 mutants (Table 3). Notably, the complementary rNTP binding affinity of Y766A is greater than that of WT or Y766F.

The T(+1)2-AP fluorescence changes for Y766F and Y766A with mispaired dNTPs were, for the most part, similar to those observed with the WT (Figure 4), though some differences were apparent, e.g., for G-dGTP and T-dGTP mispairs with Y766F, and the A-dATP and C-dATP mispairs and all mispairs at template G with Y766A. In Figure 4, all the panels have the same scale on the vertical axis (3 V total in every case) so that relatively small differences between individual base pairs are not overemphasized in experiments where the overall fluorescence changes cover a small range (e.g., Y766A, template A or T). These small differences may not be meaningful because of fluctuations in the lamp intensity during the hour or more required to collect all the traces for a particular combination of polymerase and template base. It is also difficult to make comparisons between data in different panels of Figure 4 because each set of fluorescence traces is collected at a PMT voltage appropriate for the range of that particular experiment. The stopped-flow observations in Figure 4 were therefore supplemented by steady-state measurements of fluorescence emission spectra (Figure S5 of the Supporting Information) that confirmed the trends seen in the stopped-flow data. Because the instrument settings were the same for the entire series of spectra obtained with each DNA template base, we could identify obvious outliers, for example, the high 2-AP fluorescence when Y766F binds the G-dGTP mispair and the lower fluorescence of Y766A binary complexes with the template A and G DNAs, largely accounting for the differences seen in the corresponding Y766A stopped-flow experiments.

Requirement of E710 for Step 2.1. The absence of the E710 side chain, in the E710A mutant, has a profound effect on the outcome of step 2.1 and the distinction between complementary and mismatched dNTPs. At A and C template bases, binding of the complementary dNTP results in a T(+1)2-AP fluorescence change indistinguishable from the fluorescence changes seen with mismatched dNTPs with either WT or E710A (Figure 4). The E710A C-dGTP fluorescence change can be titrated (Figure 3C and Figure S3 of the Supporting Information), just as with WT and the Y766 mutants, though the binding [$K_{d(overall)}$] is much weaker (Table 3). The apparent inability of E710A to distinguish between correct and incorrect base pairs is template-specific; at G and T templates, the characteristic step 2.1 fluorescence increase is observed, though high dNTP concentrations are required (Figure 4).

The more conservative E710Q mutation showed a phenotype intermediate between WT and E710A and was not studied in detail. At template C, binding of the complementary dGTP caused a fluorescence increase (as with WT), though the rate and binding affinity were lower (Table 3 and Figure S6 of the Supporting Information). However, as with E710A, the complementary ribonucleotide caused a fluorescence decrease similar to that observed with mismatched dNTPs (compare Figure 4 and Figure S6 of the Supporting Information).

The Closed Ternary Complex Is Not Formed in the Presence of Mispaired dNTPs. Our previously described FRET-based assay, using an AEDANS probe attached to the mobile portion of the fingers subdomain (residue 744) and a dabcyl quencher on a nonextendable DNA duplex (Figure 1), reports the fingers-closing conformational change.[17,18] The experiments depicted in Figure 8 and Figure S7A,B of the Supporting Information show that all four complementary base pairs caused the expected fingers-closing transition in WT Pol I(KF), confirming and extending the observations from our previous studies. The rates of the fingers-closing FRET change (Table 4) fit best to a biphasic curve and, like the dNTP incorporation rates (Table 1), are fastest at templates T and G and slowest at A. Addition of any noncomplementary dNTPs, or complementary rNTPs, even at 1 mM, caused little or no change in the fluorescence signal relative to the buffer-only control (Figure 8 and Figure S7 of the Supporting Information), showing that the full fingers-closing transition does not take place with these substrates. The gradual decrease in lamp intensity that takes place over the course of the experiment (shown as a gray band in Figure 8) means that we cannot completely rule out FRET changes caused by small movements of the fingers subdomain.

dx.doi.org/10.1021/bi400837k | *Biochemistry* 2013, 52, 6258−6274

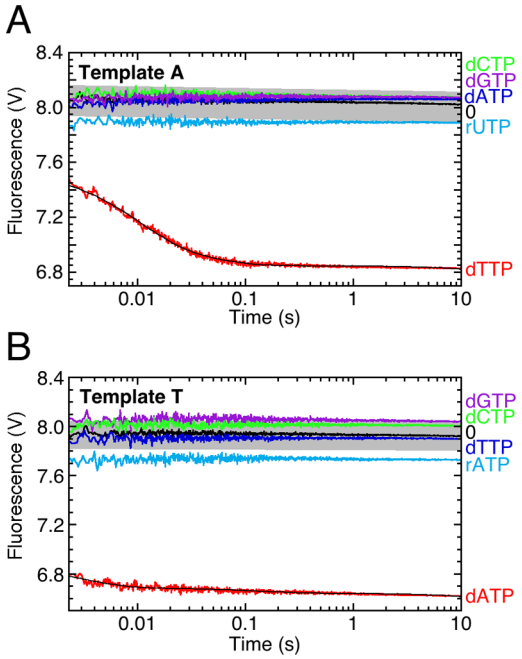

Figure 8. Fingers-closing conformational change monitored by stopped-flow fluorescence using 744-AEDANS Pol I(KF) and the dabcyl-containing DNA hairpin (Figure 2E) with a template A (A) and template T (B). The respective complementary dNTPs were present at a final concentration of 100 μM; all other nucleotides were at a final concentration of 1 mM. The black lines superimposed on the traces for the complementary dNTPs show fitting to double-exponential equations, giving the parameters reported in Table S2 of the Supporting Information. As described in Experimental Procedures, the buffer-only control was measured multiple times throughout the experiment, to track possible variations in lamp intensity. The range of the buffer-only signals is shown as a band, while the black trace, marked 0, corresponds to the average of all the determinations. To assess whether a particular nucleotide addition caused a FRET change, its stopped-flow trace was compared with buffer-only traces taken around the same time during the experiment. Intriguingly, the signal from the complementary rNTP is often at or below the lowest buffer-only signal, raising the possibility of some slight degree of fingers closing in ternary complexes with a complementary ribonucleotide.

In the experiments with G or C as the templating base, which used linear dabcyl-containing DNAs (Figure 2D), we were surprised to observe a slow (~1 s^{-1}) fluorescence decrease upon addition of mispaired dNTPs (Figure S7A,B of the Supporting Information). Further investigation (Figure S7C–F of the Supporting Information) showed that this FRET change occurred only with a linear DNA substrate and was abolished by using a multiply mutated Pol I(KF) in which binding to the 3′–5′ exonuclease site is severely compromised.[a] These observations suggest that the mispaired ternary complex, weakly bound at the polymerase active site, is in equilibrium with a species in which the other end of the linear DNA duplex interacts with the exonuclease site, bringing the quencher closer to the donor fluorophore at position 744.

Effect of Active-Site Mutations on the Fingers-Closing Step. The effect of mutations at E710 and Y766 on fingers closing is determined both by the mutation itself and, in some cases, by the identity of the base pair.

Although both Y766F and Y766A mutant proteins behaved like WT in step 2.1, their ability to execute the fingers-closing step 2.2 was markedly different. The kinetic parameters for

Table 4. Kinetic Parameters of WT and Mutant Pol I(KF) Derivatives in the FRET-Based Stopped-Flow Assay of the Fingers-Closing Conformational Change

protein	reaction[a]	k_1 (s^{-1})	k_2 (s^{-1})	$K_{d(overall)}$ (μM)
WT	A-dTTP (100 μM)	91 ± 15	23 ± 2	8.6; 11 ± 3[b]
Y766F	A-dTTP (100 μM)	58 ± 14	4.9 ± 2.2	76 ± 7
WT	T-dATP (100 μM)	410 ± 30	5.6 ± 4.3	
E710A	T-dATP (1 mM)	74 ± 12		
WT	G-dCTP (100 μM)	250		
WT	G-dCTP (10 μM)	89		
Y766A	G-dCTP (100 μM)	170		
Y766A	G-dCTP (10 μM)	65		
E710A	G-dCTP (1 mM)	79	0.34	
WT[c]	C-dGTP (10 μM)	320 ± 40	46 ± 40	

[a]The nucleotide concentrations for each reaction are in parentheses. The template A and T data were obtained using the hairpin H:T(−8)D:3′H DNA substrates (Figure 2E); the template G and C data were obtained using the linear L:T(−8)D:3′H DNA substrates (Figure 1D). Data reported as means ± the standard deviation are average values from two experiments; the others are from single determinations. Stopped-flow traces are shown in Figures 8–10 and Figures S7 and S8 of the Supporting Information. See Table S2 of the Supporting Information for a list of rate constants and amplitudes relevant to the data in this table. [b]From refs 17 and 18. [c]From ref 17.

Y766F were very similar to those of WT (Table 4), aside from ~10-fold weaker binding of the correct dNTP [measured by titration on a template A-containing substrate (Figure S8 of the Supporting Information)]. In contrast, Y766A gave no observable fingers closing with the complementary dNTP at either a template A or a template T (Figure 9A,B) even though this mutant performs step 2.1 with approximately WT kinetics (Figure 4 and Table 3). At template G, binding of dCTP caused fingers closing by Y766A and, although the amplitude of the fluorescence signal was smaller, the rate was nearly as fast as that for WT (Figure 9C,D and Table 4).

The behavior of the E710A mutant with respect to fingers closing mirrored what we observed for the preceding step 2.1 with the T(+1)2-AP probe. At template A, the complementary dTTP did not cause fingers closing, whereas the T-dATP and G-dCTP base pairs allowed fingers closing to take place [at 1 mM dNTP (Figure 10)]. It appears that the lack of the E710 side chain may not provide any additional impediment to fingers closing beyond what already exists at step 2.1.

As with WT, none of the mutant Pol I(KF) derivatives showed any detectable fingers closing with mispaired dNTPs (Figures 9 and 10).

Strong DNA Binding Correlates with the Formation of the Fully Closed Complex. The FRET-based stopped-flow fluorescence assay was adapted to measure the rates of dissociation of Pol I(KF) from binary and ternary complexes by using a non-dabcyl DNA to trap the dissociated DNA. Dissociation results in a fluorescence increase due to removal of the dabcyl quencher from the complex with the AEDANS-labeled protein (Figure 11). With WT Pol I(KF) at a template A, the presence of the complementary dTTP decreased the off-rate constant by 4–10-fold, whereas a mismatched dNTP or a complementary rNTP increased the off-rate constant by up to 10-fold, compared with that of the binary complex (Table 5). Analogous results were obtained using the T(+1)2-AP reporter (Figure S9 of the Supporting Information).

With the Y766 or E710 mutant proteins, a DNA dissociation rate slower than that of the binary complex was observed only

dx.doi.org/10.1021/bi400837k | *Biochemistry* 2013, 52, 6258–6274

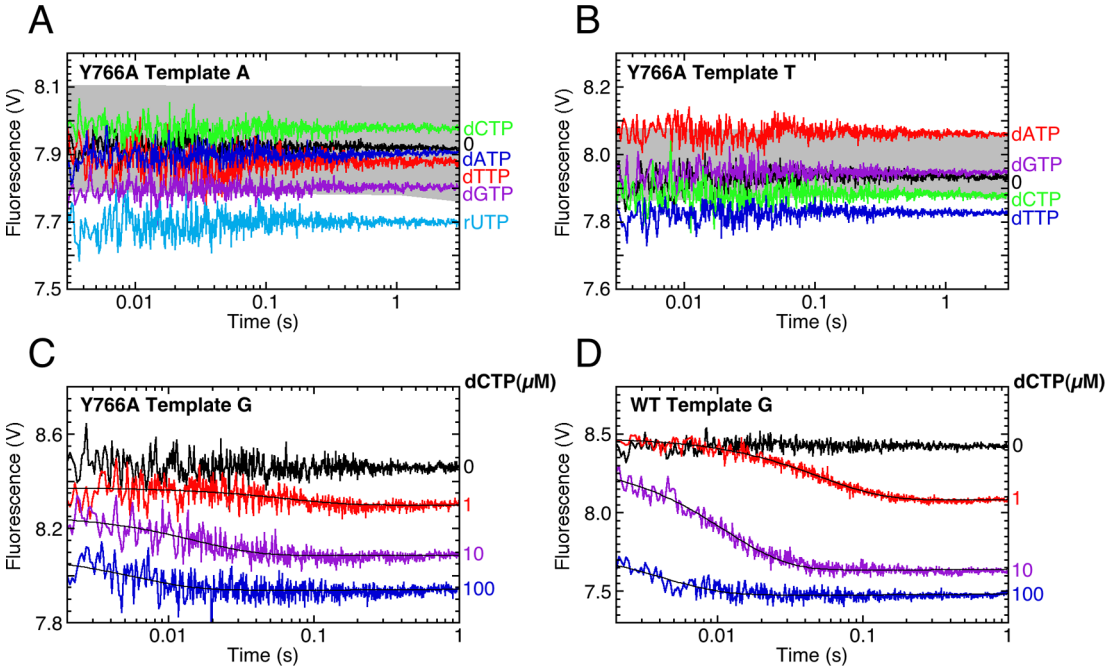

Figure 9. Stopped-flow fluorescence assay of the fingers-closing conformational change for Y766A Pol I(KF). In panels A and B, the added nucleotides were present at a final concentration of 1 mM with DNAs having templates A and T, respectively, and no fingers closing could be detected with either complementary or mismatched nucleotides. The range of the buffer-only signals is shown as a gray band, as in Figure 8. In panel C, fingers closing was observed upon binding of dCTP, at the indicated concentrations, opposite a template G. Panel D shows that a G-dCTP nascent base pair promotes fingers closing by WT Pol I(KF) at rates similar to those of Y766A. The black lines superimposed on the traces in panels C and D show fitting to single-exponential equations, giving the parameters reported in Table S2 of the Supporting Information.

under circumstances in which the closed ternary complex was formed, specifically with the Y766F A-dTTP ternary complex (Table 5). The dissociation rates for all mispaired or ribonucleotide ternary complexes were typically in the range of 20−30 s^{-1}; moreover, the correctly paired ternary complexes with the Y766A, E710A, or E710Q mutants also had dissociation rates in the mispairlike range. The dissociation rates for all Y766A complexes were higher than for the other proteins, reflecting the DNA binding defect associated with Y766A.[27]

DISCUSSION

Our two ensemble fluorescence assays provide complementary information about the prechemistry transformations that form the basis of the fidelity decisions made by Pol I(KF). The FRET-based AEDANS-dabcyl assay distinguishes open and closed conformations,[17] whereas the assay with a 2-AP probe on the DNA reports on subtle changes in the protein−DNA interactions;[16] the latter provides additional details about the earliest steps on the reaction pathway, although the structural basis of the 2-AP signal is less clear. We also consider our data in the context of single-molecule FRET studies, which use donor and acceptor probes on the protein to report the position of the fingers subdomain.[13,14]

Existence of Partially Closed Conformations. In addition to showing the open and closed conformations predicted from structural studies (Figure 1A,C), smFRET experiments detected a novel conformational species with a FRET value intermediate between those of the open and closed species.[13−15] With wild-type Pol I(KF), this intermediate-FRET species predominates in ternary complexes where the nucleotide is a noncomplementary dNTP or has the wrong sugar structure (rNTP). The observed intermediate-FRET value would correspond to movement of the mobile portion of the fingers subdomain by 20−25% of the distance along the trajectory from open to closed conformations, in excellent agreement with the partially closed mispair ternary complex structure of *Bst* DNA pol.[11] We therefore infer that an early event in the DNA polymerase reaction pathway, following the binding of any nucleotide to form a ternary complex, is the formation of a partially closed complex similar, but not necessarily identical, to the G-dTTP mispair structure (Figure 1B). With WT Pol I(KF) and a complementary dNTP, the initial partially closed complex undergoes an efficient transition to the lower-energy fully closed complex, as indicated by the low K_d(dNTP) and strong binding affinity for DNA. In mispaired or ribonucleotide complexes, the fully closed complex is destabilized and, therefore, the partially closed complex remains highly populated (provided that the dNTP concentration is high); this partially closed state is characterized by a high K_d(dNTP) (Table 3 and ref 14) and a DNA interaction that is weaker than in the Pol−DNA binary complex [shown by k_{off} values (Table 5)]. Although our current FRET probes do not distinguish different types of partially closed complex, the T(+1)2-AP probe has allowed us to dissect this population further, showing that the precise structure of the partially closed conformation depends on the nature of the incoming nucleotide, as described below.

How do we reconcile the idea of a partially closed complex as the predominant species in a mispaired or ribonucleotide ternary complex, with our ensemble, FRET-based, fingers-closing assay that shows little or no change upon addition of a mispaired dNTP (or a complementary rNTP) to the Pol I(KF) binary complex (Figure 8 and Figure S7 of the Supporting Information)? Close examination of our most recent smFRET data provides an explanation. The binary complex typically

dx.doi.org/10.1021/bi400837k | *Biochemistry* 2013, 52, 6258−6274

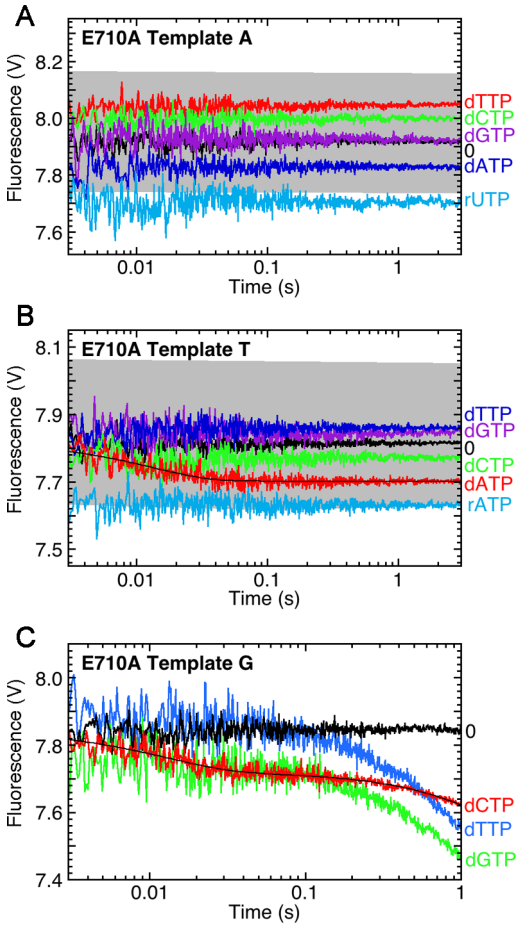

Figure 10. Stopped-flow fluorescence assay of the fingers-closing conformational change for E710A Pol I(KF). All nucleotides were present at a final concentration of 1 mM. In panel A, no fingers closing could be detected for any nucleotide opposite a template A. In panels B and C, the complementary nucleotide promoted fingers closing at templates T and G. The range of the buffer-only signals is shown as a gray band in panels A and B, as in Figure 8. In panel C, the template G DNA was a linear duplex (Figure 2D), and therefore, mismatched dNTPs caused the slow FRET decrease that we have observed in other experiments using linear DNAs (see the text and Figure S7 of the Supporting Information). The black lines superimposed on the traces for complementary dNTPs in panels B and C show fitting to exponential equations, giving the parameters reported in Table S2 of the Supporting Information.

shows 15−20% occupancy of the closed conformation; this decreases to ≲10% when the partially closed conformation becomes populated upon addition of a mispaired dNTP.[14] As a result, the population-average FRET changes very little on going from the binary complex to a mispaired ternary complex and, in an ensemble measurement, would be impossible to distinguish from signal intensity fluctuations due to lamp drift. This situation illustrates very clearly the limitations of using ensemble fluorescence measurements to report relatively subtle changes, especially in complex molecular populations.

The 2-AP Fluorescence Elucidates Early Steps on the Reaction Pathway for WT Pol I(KF) with Complementary dNTPs. Examining all four correct base pairs has greatly improved our understanding of the fluorescence changes reported by the T(+1)2-AP probe. The key observation involved template A, where addition of dTTP caused the 2-AP fluorescence to decrease and then increase (Figure 4), showing that there must be two processes, each with a characteristic effect on the environment of the 2-AP probe,[b] in the reaction at template A and, by analogy, at the other three template bases. In a previous study using a template C,[18] we had assumed that the observed rapid fluorescence increase resulted from a single 2-AP fluorescence transition on the pathway from binary to ternary complex and, therefore, that the detectable part of the fluorescence change was the latter part of a process that started within the instrument dead time. We therefore fitted the fluorescence traces to include the missing amplitude, resulting in very fast rates ($\geq$400 s^{-1}) for the T(+1)2-AP fluorescence change. Recognizing that this assumption is incorrect, here we have simply fitted the observed fluorescence traces to exponential equations and assigned the missing amplitude to a rapid initial step that takes place entirely within the instrument dead time. We were encouraged by similarities in the fitted rates from the T(+1)2-AP probe to reaction rates obtained using other experimental approaches.

First, we note that the extremely rapid T(+1)2-AP fluorescence change (the missing amplitude) may report the same step as that detected within the instrument dead time with a T(0)2-AP probe (templating base).[16] Because the fluorescence of 2-AP within DNA is quenched by stacking with its immediate neighbors,[26] this initial step would therefore involve a structural transition that simultaneously causes the templating base to become more stacked and its 5′ neighbor to become less stacked (in the case of templates C, G, and T, but not A). If one considers the structural transition from the open complex (Figure 1A,D) to the partially closed complex (Figure 1B,E), the increased level of stacking of the templating base (magenta) on the primer-terminal base pair is apparent. The structural basis for the fluorescence changes of the T(+1) base (cyan) may be more complex, as suggested by the strong influence of the nature of the templating base (discussed below).

Following the dead time fluorescence change, the subsequent T(+1)2-AP fluorescence transitions (corresponding to the first and second fitted rates) give rates similar to the measured fingers-closing and dNTP incorporation rates, respectively (compare k_1 in Tables 3 and 4 and k_2 in Table 3 with k_{pol} in Table 1). Moreover, there is a consistent correlation such that situations that show a rapid k_1 with the T(+1)2-AP probe also show a rapid fingers-closing k_1; compare, for example, the four correct base pairs with WT Pol I(KF), the results with mutant proteins in this study, and the D705A mutant in a previous study.[18] One possible explanation is that the two stopped-flow assays report the same process, fingers closing coupled with a change in the environment of the T(+1) base. However, we have observed situations in which the two processes are decoupled, giving a robust T(+1)2-AP fluorescence increase but no fingers closing; these are the D882A mutant[18] and, in the study presented here, several reactions with complementary rNTPs. We therefore favor the alternative explanation that fingers closing is fast but the DNA rearrangement step is required before fingers closing can take place. As a result, fingers closing will be kinetically invisible and rate-limited by the DNA rearrangement step.[c] In either stopped-flow assay, the k_1 fluorescence increase would then be augmented at a slower rate, k_2, as the following reaction steps displace the equilibrium toward products. The similarity of k_2 to the dNTP incorporation rate suggests that k_2 reflects rate-limiting step 3 of the pathway (Figure 12).

dx.doi.org/10.1021/bi400837k | Biochemistry 2013, 52, 6258−6274

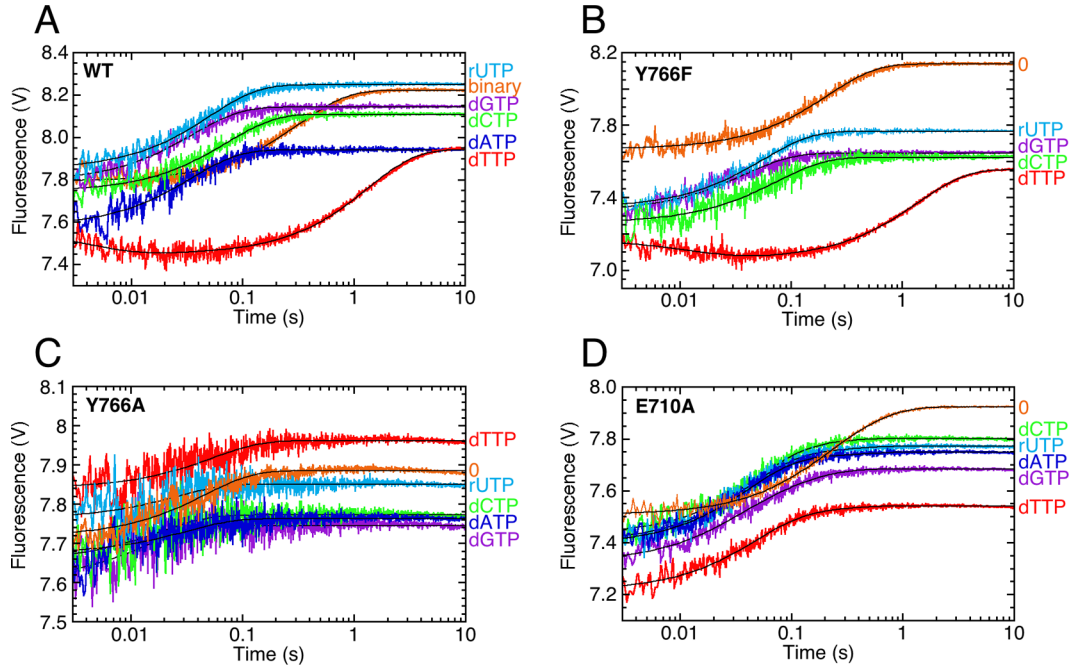

Figure 11. DNA dissociation measured by stopped-flow fluorescence using the FRET-based assay with 744-AEDANS Pol I(KF) and the T(−8)dabcyl DNA hairpin with templating base A (Figure 2E), for WT and mutant proteins, as indicated in each panel. Addition of an excess of an unmodified DNA duplex to serve as a trap prevented reassociation of the original Pol−DNA binary complex, resulting in a fluorescence increase. Throughout, the orange trace shows the dissociation of the Pol−DNA binary complex without additional dNTPs. The other traces show the dissociation of ternary complexes, measured by including 2 mM complementary or mismatched deoxynucleotide, or a complementary ribonucleotide, in the DNA trap solution. The rates of dissociation are listed in Table 5. The black lines superimposed on the traces show fitting to single- or double-exponential equations, giving the parameters reported in Table S2 of the Supporting Information (see Figure S3B of the Supporting Information for an example of curve fitting and residuals).

Table 5. DNA Dissociation Rates Obtained from the FRET-Based Assays in Figure 11, with A as the Templating Base

	k_{off} (s^{-1})[a]				
nucleotide[b]	WT	Y766F	Y766A	E710A	E710Q
none[c]	3.1 ± 0.2	4.5 ± 0.2	17 ± 7	6.5 ± 1.0	2.6 ± 0.3
dTTP	0.80 ± 0.07	0.68 ± 0.07	27 ± 11	26 ± 6	13 ± 4
dATP	29 ± 0.4		32	29 ± 6	17
dCTP	14 ± 0.14	13	55	24 ± 3	9.6
dGTP	26 ± 3	28 ± 2	59 ± 21	33 ± 7	15 ± 8
rUTP	19 ± 0.3	18	52 ± 18	26 ± 2	12 ± 5

[a]Using the dabcyl-containing H:T(−8)D:3′H DNA and the indicated 744-AEDANS Pol I(KF) derivatives. Most of the rate constants were determined by fitting the fluorescence increase to a single exponential. The traces for WT and Y766F with the correct nucleotide (dTTP) were fit to double exponentials because of the initial rapid fluorescence decrease due to fingers closing. The traces for E710A were fit to a double exponential to take into account a second slow phase; only the rates of the predominant first phase are reported here. See Table S2 of the Supporting Information for a list of rate constants and amplitudes relevant to the data in this table and Figure S3B of the Supporting Information for an example of curve fitting and residuals. Data reported as means ± the standard deviation are average values from two experiments; the others are from single determinations. [b]The indicated nucleotide (2 mM) was present in the syringe with the unmodified trap DNA, giving a final concentration of 1 mM in the stopped-flow cell. [c]Corresponds to dissociation from the Pol−DNA binary complex.

A Structural Description of Early Steps of the Reaction Remains Elusive. The T(+1)2-AP probe reveals distinct conformational intermediates within the population of putative partially closed complexes early in the Pol I(KF) reaction pathway. However, deducing structural transitions from the observed fluorescence changes is extremely challenging, and we therefore use the T(+1)2-AP fluorescence signal empirically, as an identifier for distinct species on the reaction pathway rather than an indication of their structures.

The template strands used in these experiments differ in only one position, the templating base, 3′ to the 2-AP probe. In the absence of protein, the fluorescence of these DNAs, whether single-stranded or annealed to a primer strand, roughly follows the expectation that purine neighbors would stack more effectively than pyrimidines (Figure 5).[d] When 2-AP is bound to Pol I(KF), the fluorescence at both the T(0) and T(+1) positions is greatly enhanced,[16] consistent with binary complex cocrystal structures showing that the interaction between the T(0) and T(+1) bases is disrupted (Figure 1A,D). The different fluorescence signals of T(+1)2-AP in the four binary complexes (Figure 5) are somewhat surprising and imply variability in the interaction between the T(+1) base and the four templating bases.[e] Structurally, we could envisage the template bases A, C, G, and T being sequestered in the pocket between helices O and O_1 to differing extents, with A being the most buried (therefore least available for stacking) and G the

dx.doi.org/10.1021/bi400837k | Biochemistry 2013, 52, 6258−6274

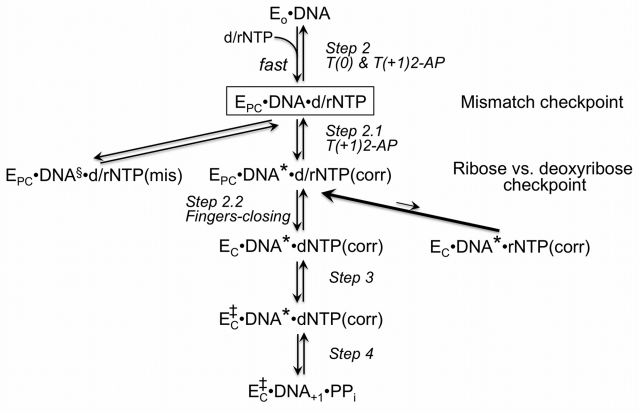

Figure 12. Revised reaction pathway for Pol I(KF) from DNA binding to phosphoryl transfer, showing the proposed common ternary complex intermediate (boxed), whose subsequent transformations lead to different fates for mispaired dNTPs, complementary ribonucleotides, and complementary dNTPs. E_O, E_{PC}, and E_C represent the open, partially closed, and fully closed conformations, respectively, of the polymerase fingers subdomain. The fluorescent probes diagnostic of each of the early steps are indicated. DNA* represents the DNA rearrangement that results in a fluorescence increase of the 2-AP probe 5′ to the templating position; DNA§ represents the alternative rearrangement that takes place with a mispaired nucleotide. E_C to $E_C^{\ddagger}$ (step 3) is a transformation, probably involving entry of a divalent metal ion, that assembles the active site for catalysis;[18] this step is rate-limiting for addition of a single complementary dNTP. The existence of additional, as yet undetected, steps cannot be ruled out.

least. However, because smFRET data show the binary complex to be a mixture of open and closed conformations,[13,14] a more likely explanation is that the identity of the T(0) base could influence the conformational distribution of the binary complex. Compared to the binary complex, the correctly paired closed ternary complex has much less structural variability, judging from the similar T(+1)2-AP fluorescence emission regardless of the identity of the T(0) base (Figure 5A). The high fluorescence of the correctly paired ternary complex, implying minimal interaction between the T(0) and T(+1) bases, is as expected from cocrystal structures of *Bst* DNA pol (Figure 1C,F) and many other DNA polymerases,[6−9] in which the T(+1) base is completely dislocated from the T(0) base and the primer-terminal duplex.

On the basis of their T(+1)2-AP fluorescence signals, mispaired ternary complexes can be divided into two classes. Mispaired ternary complexes with template pyrimidines have fluorescence emission that is similar to that of the corresponding binary complex, whereas those with template purines have lower fluorescence (Figures 4 and 5B), suggesting more structural reorganization (with an increased level of quenching of the 2-AP probe) upon formation of a Pu-dNTP mispair. As with the binary complex (discussed above), the difference between the categories could be purely physical (two distinct structural classes) or temporal, with the templating base influencing the equilibrium between high- and low-fluorescence conformational states. In Figure 5B, which shows the mispair with the lowest fluorescence emission at each template base, the templating G is the most effective quencher of T(+1)2-AP, just as in the unbound duplex DNA. Interestingly, the fluorescence signals from G-dCTP (closed) and G-dTTP (partially closed) complexes are quite different, despite the apparently similar environments of the T(+1) base in the corresponding cocrystal complexes (Figure 1E,F and ref 11). If, as suggested above, the mispair complex were a conformationally mixed population, this complexity would probably not be captured in a cocrystal. Furthermore, we should not necessarily take the G-dTTP complex structure as a universal model for mispair ternary complexes. The degree of engagement of the templating base with the incoming nucleotide, and the extent of its stacking on the primer-terminal base pair, are likely to be determined by the identity of the nascent base pair. The geometry of G-dTTP may be particularly compatible with the polymerase active site, and one should not necessarily expect the same for Pu-dPuTP, Py-dPyTP, or even the opposite orientation wobble mispairs, Py-dPuTP. Given the exceptional versatility of *Bst* DNA pol in generating interesting cocrystal structures, we must hope that other mispaired ternary complex structures will be determined in the future.

A Branched Reaction Pathway Governs Nucleotide Selection by Pol I(KF). In Figure 12, we have updated the polymerase reaction pathway of Pol I(KF)[17,18] to incorporate new information from the current study and to indicate the alternative pathways followed by mispair and ribonucleotide ternary complexes.

We propose that all nucleotides cause the open binary complex to undergo a transition (in step 2) to a common intermediate (boxed in Figure 12), probably a partially closed state. This first binding event is extremely rapid and corresponds to the 2-AP fluorescence changes at T(0) or T(+1) that take place within the dead time of the stopped-flow instrument. While it is easy to envisage a common early intermediate in the dead time T(+1)2-AP signals observed upon binding of a complementary dNTP or rNTP (Figures 4 and 6), the case for an analogous intermediate with mispaired dNTPs is more speculative. Nevertheless, in support of this idea, we note that the majority of the mispair traces in Figure 4 have a concave-up shape and could plausibly be the tail end of processes originating at a fluorescence higher than the observed vertical axis intercept. We would not necessarily expect all the traces for a particular template base to emanate from the same fluorescence value because the equilibrium between the binary complex and the proposed common intermediate may be less favorable for some mispairs, resulting in a smaller fluorescence change upon binding of the mispaired dNTP.

Within the initial partially closed ternary complex, there must be an interaction that allows the incoming nucleotide to preview the templating base; this could be a configuration resembling that seen in the *Bst* DNA pol mismatch ternary complex (Figure 1E), but with the precise geometry of the nascent mispair dictated by the type of mispair being formed. This first complex constitutes the most important checkpoint on the reaction pathway, in that it is where noncomplementary nucleotides are identified and diverted, at step 2.1, toward a mismatch-specific outcome, resulting in a family of complexes that are distinguishable, by their much lower T(+1)2-AP fluorescence, from those formed by complementary nucleotides.

Complementary nucleotides (both ribo and deoxyribo) undergo a different conformational transition at step 2.1, signaled by a further increase in the fluorescence of the T(+1)2-AP probe. The subsequent fingers-closing step 2.2 is the second checkpoint on the pathway; with deoxynucleotides, the equilibrium favors the forward reaction, whereas the steric constraints associated with the 2′OH of a ribonucleotide

dx.doi.org/10.1021/bi400837k | *Biochemistry* 2013, 52, 6258−6274

destabilize the closed conformation, making the equilibrium of this step unfavorable and trapping the rNTP ternary complex at the partially closed state.[12] Thus, the step 2.1 and 2.2 checkpoints ask successive binary questions: Is the nucleotide complementary to the template, and is the sugar a deoxyribose? Only when the answers to both questions are "yes" does a WT Pol I(KF) ternary complex undergo an efficient transition to the immediate prechemistry state (where, in our experiments, it is arrested because of the absence of the primer 3′OH). Formation of the fully closed ternary complex increases the binding affinity of both dNTP and DNA; successful transit through step 2.1 (e.g., for WT with complementary rNTPs) is not sufficient to provide strong DNA binding. The favorable equilibrium across step 2.2 for correctly paired dNTP complexes will also displace the equilibrium of the earlier steps, amplifying their fluorescence signals (e.g., compare dGTP and rGTP traces in Figure 6A).

With the exception of the complex with the complementary dNTP, all other ternary complexes are trapped as a population consisting primarily of partially closed complexes, characterized by weaker binding of both DNA and nucleotides, which should facilitate dissociation and further attempts to bind the correct dNTP. Although the ternary complexes of mispairs and complementary ribonucleotides are both effectively arrested at the partially closed state, they clearly have different physical characteristics as shown by the T(+1)2-AP signal. The same conclusion was reached in a study using an entirely different physical technique based on the properties of single Pol I(KF) complexes associated with α-hemolysin nanopores.[30] Although both incorrect dNTPs and complementary rNTPs can be incorporated into DNA, their incorporation rates are slower than those of complementary dNTPs by at least 500-fold. This rate difference represents the combination of (1) inefficient progress through the prechemistry steps and (2) a geometrically compromised transition state that slows the rate of phosphoryl transfer to the point where this step becomes rate-limiting.

Mutator Mutants Affect the Early Checkpoints. Our inference that the early checkpoints are implicated in fidelity is supported by the observation that they are compromised in mutator mutants Y766A and E710A. In WT Pol I(KF), the net result of the two early checkpoints is that a ternary complex with a complementary dNTP is uniquely directed to the fully closed complex. Both E710A and Y766A are less effective in routing at least a subset of the correct nascent base pairs toward the closed complex. As a result, the early checkpoints operate with a lower specificity and a larger proportion of errors pass through the checkpoints.

E710A Affects the Step 2.1 Checkpoint. On the basis of the T(+1)2-AP signal, we infer that E710A fails to recognize A-dTTP and C-dGTP as correct nascent base pairs. Instead of the normal step 2.1 DNA rearrangement, these base pairs undergo a transition resembling the mispair-specific step 2.1 (Figure 4). With G-dCTP and T-dATP base pairs, the normal step 2.1 fluorescence change is observed but much higher dNTP concentrations are required, indicating that the product of step 2.1 is destabilized relative to the situation with WT Pol I(KF). Nevertheless, the G-dCTP and T-dATP products after step 2.1 are able to proceed through step 2.2 (fingers closing), suggesting that there is no subsequent defect in fingers closing due to the E710A mutation. Structural studies of the equivalent mutant of *Bst* DNA pol (E658A) could not capture a G-dCTP nascent base pair at the active site,[12] consistent with the weaker binding of complementary dNTPs by E710A Pol I(KF) (this study and refs 14, 23, and 24). These same structural studies noted the absence in E658A *Bst* DNA pol of an active-site water molecule, which is normally present in all A-family DNA polymerase complexes.[6,12,31] This water molecule is coordinated by three invariant active-site side chains [E710, N845, and Q849 in Pol I(KF)] and interacts with the minor groove of the nascent base pair; its absence could potentially affect nucleotide binding in the complexes that play a role in the early fidelity checkpoints.

The base specificity of the E710A phenotype is puzzling: Why should T-dATP and G-dCTP base pairs be less affected than A-dTTP and C-dGTP base pairs? It would be easy to rationalize a distinction between A/T and G/C pairings, based on the hydrogen-bonding strength of the nascent base pair, or between purines and pyrimidines as the incoming nucleotide, based, for example, on whether N_3 (purines) or O_2 (pyrimidines) were available to interact with the active-site water molecule mentioned above. The observed preference by E710A for T-dATP and G-dCTP roughly parallels some properties of WT Pol I(KF) at templates T and G: higher dNTP incorporation rates (Table 1) and more robust T(+1)2-AP fluorescence changes upon binding of the complementary rNTP (Figure 5B). Thus, the bias in favor of templates T and G might be inherent to this particular polymerase active site, and the differences in reaction kinetics are merely exacerbated by mutation of a critical active-site residue. An important caveat is that DNA polymerase behavior, reflected in measurable properties such as processivity or fidelity, is strongly influenced by sequence context.[21] If the rate constants of individual reaction steps are similarly influenced, one might not necessarily find the identical base pair preferences in a different DNA sequence.

The Y766 Side Chain Primarily Affects Fingers Closing (step 2.2). The Y766F and Y766A mutations have very little effect on the T(+1)2-AP fluorescence signals from the majority of ternary complexes in step 2.1 (Figure 4). The few differences observed for mispaired complexes (e.g., the higher fluorescence signal for G-dGTP with Y766F) could indicate either that mutation of Y766 alters the DNA conformation around the templating base in particular complexes or that the DNA conformation is the same but the mutated 766 side chain affects the 2-AP fluorescence signal. In contrast with E710A, Y766A strongly influences step 2.2, with no fingers closing detectable in our assay for A-dTTP and T-dATP base pairs, although fingers closing is similar to that of WT for G-dCTP base pairs. The smFRET data for Y766A support these observations, showing that, for A-dTTP and T-dATP, the partially closed and fully closed complexes are isoenergetic, whereas the fully closed G-dCTP complex is stabilized, just as in the WT enzyme.[14] As with E710A, we do not have an explanation for this base pair specificity.

In the partially closed *Bst* DNA pol complexes,[11] helix O is kinked such that residues close to the C-terminus occupy positions very similar to those in the fully closed complex. The side chains equivalent to Y766 and F762 (Y714 and F710) point toward the active-site cleft, abutting one another and forming a substantial part of the binding pocket for the nascent base pair. In the Y714S mutant of *Bst* DNA pol [which we assume to be a reasonable model for Pol I(KF) Y766A], the F710 side chain is differently positioned and this, together with the smaller size of the side chain at position 714, significantly changes the shape of the active-site pocket (Figure 13). The

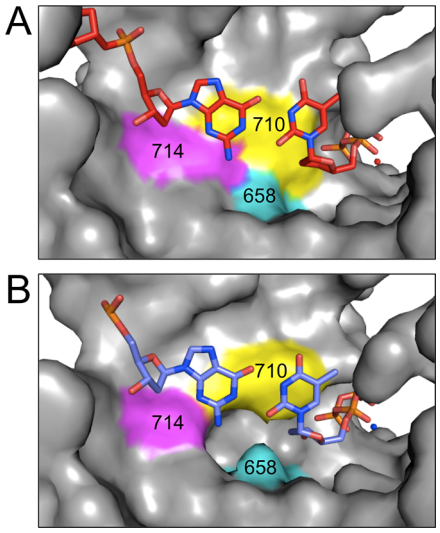

Figure 13. Structural changes associated with the Y766A mutation, inferred from *Bst* DNA pol cocrystal structures. The panels show ternary complexes with a nascent G-dTTP mispair at the active site, and the protein in the partially closed conformation.[11] The protein is shown as a surface representation, with the positions of *Bst* DNA pol side chains 714, 710, and 658 colored magenta, yellow, and cyan, respectively; in Pol I(KF), the equivalent side chains are 766, 762, and 710, respectively. (A) Active site with Tyr at position 714 (766) (from PDB entry 3HP6). (B) Active site in the Y766S mutant (from PDB entry 3HPO). [Note that the protein in panel A is the F710Y mutant whereas the protein in B has the wild-type Phe at position 710. A comparison of structures that differ only in having F or Y at position 710 (e.g., PDB entries 1LV5 and 2HVI, refs 8 and 39) indicates that this change does not account for the active-site differences illustrated here.] This figure was made using PyMOL (Schrödinger, LLC).

loss of these inter-side chain contacts could change the relative stabilities of open, partially closed, and fully closed conformations, influencing the energy profile of the early checkpoint steps. Although the Y766A mutation creates space in the active site that could potentially accommodate noncomplementary pairings, we see no evidence, either in this study or in the smFRET data,[14] that Y766A processes mispairs through the early checkpoints in a manner that is different from that of the WT enzyme. The data point to a deficiency in singling out certain correct base pairs for preferential treatment, resulting in an overall increase in the frequency of errors that pass through steps 2.1 and 2.2. The more spacious active site may, however, play a role in the subsequent steps of misincorporation as shown by the more favorable kinetics (relative to that of WT) of some misinsertion reactions of Y766S.[20]

Phenotype of Y766F. Unlike Y766A, the conservative Y766F mutation has very little effect on the kinetics of fingers closing. Thus, the Y766−E710 hydrogen bond does not appear to stabilize the fully closed complex. smFRET studies support this conclusion, showing that, in the unliganded protein, Y766F actually favors the closed conformation whereas WT is biased slightly toward the open conformation. Our explanation is that the hydrophobic phenylalanine side chain destabilizes the open conformation because of the extremely solvent-exposed environment of the 766 residue. Because the relatively mild phenotype of Y766F argues against the Y766−E710 hydrogen bond being a necessary feature of Y766, perhaps its purpose is to fix the position of E710. Mispositioning, or increased mobility, of E710 could account for the subtle changes associated with the Y766F mutation: weaker dNTP binding and slight changes in the handling of rNTPs in the early steps (Table 3 and Figure 6).

Given that the Y766F mutant shows very little difference from WT in terms of reaction kinetics, fidelity, and other properties that have been examined in this and previous studies,[20,21,32] it is perhaps surprising that tyrosine is invariant at this position in A-family DNA polymerase sequences.[33,34] The corresponding Y-to-F substitution was observed in a localized mutagenesis experiment on *Taq* DNA polymerase that involved a short selection *in vivo*,[35] implying that the defect associated with the Y766F substitution is indeed mild but that this allele would eventually be eliminated during growth in the wild. Our data suggest that Y766F is associated with a small decrease in the level of discrimination against rNTPs, too small to be detected in an earlier screen for rNTP incorporation.[24] This behavior of Y766F could plausibly confer a small selective disadvantage, given the excess of rNTPs over dNTPs *in vivo* and the deleterious consequences of incorporation of rNTPs into DNA.[3,4,36]

Error Specificity of the E710A and Y766A Mutator Polymerases. As described above, the E710A and Y766A mutators are impaired in the processing of at least a subset of correct base pairs, making the early checkpoints less effective in screening out mispairs so that a higher frequency of these errors can be recovered as mutations using an appropriate indicator gene (Table 6). The base pair-specific effects we describe predict that E710A should be more accurate at templates G and T than at templates A and C, and that Y766A should be inaccurate at templates A and T but have approximately WT fidelity at template G, where the kinetic parameters are similar to those of WT. In Table 6, which shows the frequencies of mutations resulting from all 12 possible mispairs for WT, E710A, and Y766A, the aggregate mutation frequencies at each template base (fourth entry for each template base) are broadly consistent with the expectations from our biochemical analysis. The notable exception involves E710A at template C where our data predict a substantially higher error rate.[†]

We would not necessarily expect the behavior of polymerases at the early checkpoints to account fully for the error specificities reported in Table 6. To be detected as a mutational end point, a mispaired dNTP must not only pass through the early checkpoints but also be covalently incorporated onto the DNA primer followed by extension of the resulting mismatch. The constraints of active-site geometry in these later steps of the reaction pathway will result in mispair-specific preferences that determine which mutations are recovered at high frequency; note, for example, the predominance of mutations resulting from wobble (Pu-Py) mispairs in Table 6. In a previous study, we were able to account for aspects of the incorporation kinetics and mispair specificity of WT and E710A Pol I(KF) simply by considering mispair geometry relative to the closed complex active-site pocket.[23]

This study suggests that a common feature of mutator polymerases is the impaired recognition of complementary base pairs as "correct", diminishing the overall effectiveness of the early checkpoints. The mutator alleles that affect these early transitions will also influence the interactions between nascent mispairs and the polymerase active site in later steps of the reaction, determining the characteristic mutational repertoire of each mutator.

Table 6. Frequencies of Individual Base Substitution Errors Made by E710A and Y766A Pol I(KF) Mutants[a]

mispair[b]	WT mutants	E710A mutants	error rate,[c] E710A:WT	Y766A mutants	error rate,[c] Y766A:WT
A-dCTP	1	51	75	6	21
A-dATP	2	7	5.1	5	8.8
A-dGTP	0	0		5	
A-dXTP	**3**	**58**	**28**	**16**	**19**
T-dGTP	19	14	1.1	55	10
T-dTTP	1	6	8.8	0	0
T-dCTP	6	18	4.4	0	0
T-dXTP	**26**	**38**	**2.1**	**55**	**7.5**
G-dTTP	2	14	10	7	12
G-dGTP	10	1	0.1	1	0.4
G-dATP	10	3	0.4	2	0.7
G-dXTP	**22**	**18**	**1.2**	**10**	**1.6**
C-dATP	13	7	0.8	1	0.3
C-dCTP	0	0		0	
C-dTTP	0	2		0	
C-dXTP	**13**	**9**	**1.0**	**1**	**0.3**
total	94	135		103	
MF ($\times 10^{-4}$)	57	120		220	

[a]Polymerase errors were measured in a forward mutational assay using the *lacZα* gene in a phage M13mp2 vector.[37] The table lists the number of *lacZ* mutants, recovered after gap-filling synthesis by each of the indicated polymerases, that result from individual mismatch errors. The data for WT and E710A Pol I(KF) are from ref 23, and the data for Y766A are from ref 21. [b]The fourth entry of each set (bold) is the total number of *lacZ* mutants resulting from mispairing at the indicated template base (A, C, G, or T). [c]The frequency of each type of base substitution error is calculated by multiplying the overall mutant frequency (MF) by the proportion of mutants of each type (as a fraction of the total number of mutants recovered). Correction factors for the expression of errors on transfection, and for the number of detectable sites for each type of mutation, cancel out when calculating the ratio of error frequencies for mutant and WT polymerases.

■ ASSOCIATED CONTENT

Supporting Information

Additional chemical quench data (Figures S1 and S2), stopped-flow fluorescence data (Figures S3, S4, and S6−S9), fluorescence emission data (Figure S5), amplitudes and rate constants corresponding to the fitted curves throughout this study (Tables S1 and S2). This material is available free of charge via the Internet at http://pubs.acs.org.

■ AUTHOR INFORMATION

Corresponding Author

*Department of Molecular Biophysics and Biochemistry, Yale University, Bass Center for Molecular and Structural Biology, 266 Whitney Ave., P.O. Box 208114, New Haven, CT 06520-8114. E-mail: catherine.joyce@yale.edu. Phone: (203) 432-8992. Fax: (203) 432-5175.

Present Address

[†]O.B.: Lineberger Comprehensive Cancer Center, University of North Carolina, Chapel Hill, NC 27599.

Funding

This work was supported by National Institutes of Health Grant GM-28550.

Notes

The authors declare no competing financial interest.

■ ACKNOWLEDGMENTS

We are grateful to Olga Potapova for invaluable technical support and Enrique De La Cruz and Anna M. Pyle for the use of their stopped-flow instruments.

■ ABBREVIATIONS

Pol I(KF), Klenow fragment of *E. coli* DNA polymerase I; *Bst* DNA pol, portion of *B. stearothermophilus* DNA polymerase equivalent to Klenow fragment; smFRET, single-molecule fluorescence resonance energy transfer; 2-AP, 2-aminopurine; IAEDANS, 5-{[(2-iodoacetyl)amino]ethyl}aminonaphthalene-1-sulfonic acid; dNTP, deoxynucleoside triphosphate; WT, wild-type; PDB, Protein Data Bank; PMT, photomultiplier tube.

■ ADDITIONAL NOTES

[a]A previously published experiment,[17] using a linear DNA with template C, did not show the slow fluorescence decrease because the multiply mutated polymerase was used.

[b]Because the template A substrate shows an immediate fluorescence decrease followed by a fluorescence increase, the latter must derive from an actual change in the environment of the T(+1)2-AP probe. Conversely, in situations where we observe a biphasic fluorescence increase, we cannot rule out the possibility that only the first step gives rise to the fluorescence signal, and the subsequent slower step merely augments the signal by shifting the equilibrium toward products.

[c]This is analogous to the way in which the chemical step of phosphoryl transfer is rate-limited by the preceding non-covalent step[28] and, just as in this case, one might expect to find mutations or other circumstances that slow fingers closing to the point where it becomes kinetically observable.

[d]The effect of the neighboring base on the fluorescence intensity in our study is different from the published report for 2-AP within a duplex DNA environment.[29]

[e]There is no correlation between the binary complex fluorescence and the fluorescence of the unbound DNA duplex, ruling out the possibility that the structural character of the DNA is preserved in the binary complex.

[f]An important caveat is that the WT number of C-dATP errors could be inflated by C-to-U depurination on the template strand. Because of the low frequency of mutants recovered from the WT polymerase, rare events of this type are more likely to be represented in the WT data, leading to an underestimate of the C-dATP error rate for the mutator polymerases.

■ REFERENCES

(1) Kunkel, T. A., and Bebenek, K. (2000) DNA replication fidelity. *Annu. Rev. Biochem. 69*, 497−529.

(2) Joyce, C. M., and Benkovic, S. J. (2004) DNA polymerase fidelity: Kinetics, structure, and checkpoints. *Biochemistry 43*, 14317−14324.

(3) Traut, T. W. (1994) Physiological concentrations of purines and pyrimidines. *Mol. Cell. Biochem. 140*, 1−22.

(4) Nick McElhinny, S. A., Watts, B. E., Kumar, D., Watt, D. L., Lundström, E. B., Burgers, P. M., Johansson, E., Chabes, A., and Kunkel, T. A. (2010) Abundant ribonucleotide incorporation into

DNA by yeast replicative polymerases. *Proc. Natl. Acad. Sci. U.S.A. 107*, 4949−4954.
(5) Doublié, S., Sawaya, M. R., and Ellenberger, T. (1999) An open and closed case for all polymerases. *Structure 7*, R31−R35.
(6) Doublié, S., Tabor, S., Long, A., Richardson, C. C., and Ellenberger, T. (1998) Crystal structure of a bacteriophage T7 DNA replication complex at 2.2 Å resolution. *Nature 391*, 251−258.
(7) Li, Y., Korolev, S., and Waksman, G. (1998) Crystal structures of open and closed forms of binary and ternary complexes of *Thermus aquaticus* DNA polymerase I: Structural basis for nucleotide incorporation. *EMBO J. 17*, 7514−7525.
(8) Johnson, S. J., Taylor, J. S., and Beese, L. S. (2003) Processive DNA synthesis observed in a polymerase crystal suggests a mechanism for the prevention of frameshift mutations. *Proc. Natl. Acad. Sci. U.S.A. 100*, 3895−3900.
(9) Franklin, M. C., Wang, J., and Steitz, T. A. (2001) Structure of the replicating complex of a pol alpha family DNA polymerase. *Cell 105*, 657−667.
(10) Sawaya, M. R., Prasad, R., Wilson, S. H., Kraut, J., and Pelletier, H. (1997) Crystal structures of human DNA polymerase β complexed with gapped and nicked DNA: Evidence for an induced fit mechanism. *Biochemistry 36*, 11205−11215.
(11) Wu, E. Y., and Beese, L. S. (2011) The structure of a high fidelity DNA polymerase bound to a mismatched nucleotide reveals an "ajar" intermediate conformation in the nucleotide selection mechanism. *J. Biol. Chem. 286*, 19758−19767.
(12) Wang, W., Wu, E. Y., Hellinga, H. W., and Beese, L. S. (2012) Structural factors that determine selectivity of a high fidelity DNA polymerase for deoxy-, dideoxy-, and ribonucleotides. *J. Biol. Chem. 287*, 28215−28226.
(13) Santoso, Y., Joyce, C. M., Potapova, O., Le Reste, L., Hohlbein, J., Torella, J. P., Grindley, N. D. F., and Kapanidis, A. N. (2010) Conformational transitions in DNA polymerase I revealed by single-molecule FRET. *Proc. Natl. Acad. Sci. U.S.A. 107*, 715−720.
(14) Hohlbein, J., Aigrain, L., Craggs, T. D., Bermek, O., Potapova, O., Shoolizadeh, P., Grindley, N. D. F., Joyce, C. M., and Kapanidis, A. N. (2013) Conformational landscapes of DNA polymerase I and mutator derivatives establish fidelity checkpoints for nucleotide insertion. *Nat. Commun. 4*, 2131.
(15) Berezhna, S. Y., Gill, J. P., Lamichhane, R., and Millar, D. P. (2012) Single-molecule Förster resonance energy transfer reveals an innate fidelity checkpoint in DNA polymerase I. *J. Am. Chem. Soc. 134*, 11261−11268.
(16) Purohit, V., Grindley, N. D. F., and Joyce, C. M. (2003) Use of 2-aminopurine fluorescence to examine conformational changes during nucleotide incorporation by DNA polymerase I (Klenow fragment). *Biochemistry 42*, 10200−10211.
(17) Joyce, C. M., Potapova, O., DeLucia, A. M., Huang, X., Basu, V. P., and Grindley, N. D. F. (2008) Fingers-closing and other rapid conformational changes in DNA polymerase I (Klenow fragment) and their role in nucleotide selectivity. *Biochemistry 47*, 6103−6116.
(18) Bermek, O., Grindley, N. D. F., and Joyce, C. M. (2011) Distinct roles of the active-site Mg^{2+} ligands, Asp882 and Asp705, of DNA polymerase I (Klenow fragment) during the prechemistry conformational transitions. *J. Biol. Chem. 286*, 3755−3766.
(19) Polesky, A. H., Steitz, T. A., Grindley, N. D. F., and Joyce, C. M. (1990) Identification of residues critical for the polymerase activity of the Klenow fragment of DNA polymerase I from *Escherichia coli*. *J. Biol. Chem. 265*, 14579−14591.
(20) Carroll, S. S., Cowart, M., and Benkovic, S. J. (1991) A mutant of DNA polymerase I (Klenow fragment) with reduced fidelity. *Biochemistry 30*, 804−813.
(21) Bell, J. B., Eckert, K. A., Joyce, C. M., and Kunkel, T. A. (1997) Base miscoding and strand misalignment errors by mutator Klenow polymerases with amino acid substitutions at tyrosine 766 in the O helix of the fingers subdomain. *J. Biol. Chem. 272*, 7345−7351.
(22) Minnick, D. T., Bebenek, K., Osheroff, W. P., Turner, R. M., Jr., Astatke, M., Liu, L., Kunkel, T. A., and Joyce, C. M. (1999) Side chains that influence fidelity at the polymerase active site of *Escherichia coli* DNA polymerase I (Klenow fragment). *J. Biol. Chem. 274*, 3067−3075.
(23) Minnick, D. T., Liu, L., Grindley, N. D. F., Kunkel, T. A., and Joyce, C. M. (2002) Discrimination against purine-pyrimidine mispairs in the polymerase active site of DNA polymerase I: A structural explanation. *Proc. Natl. Acad. Sci. U.S.A. 99*, 1194−1199.
(24) Astatke, M., Ng, K., Grindley, N. D. F., and Joyce, C. M. (1998) A single side chain prevents *Escherichia coli* DNA polymerase I (Klenow fragment) from incorporating ribonucleotides. *Proc. Natl. Acad. Sci. U.S.A. 95*, 3402−3407.
(25) Joyce, C. M., and Derbyshire, V. (1995) Purification of *E. coli* DNA polymerase I and Klenow fragment. *Methods Enzymol. 262*, 3−13.
(26) Rachofsky, E. L., Osman, R., and Ross, J. B. (2001) Probing structure and dynamics of DNA with 2-aminopurine: Effects of local environment on fluorescence. *Biochemistry 40*, 946−956.
(27) Astatke, M., Grindley, N. D. F., and Joyce, C. M. (1995) Deoxynucleoside triphosphate and pyrophosphate binding sites in the catalytically competent ternary complex for the polymerase reaction catalyzed by DNA polymerase I (Klenow fragment). *J. Biol. Chem. 270*, 1945−1954.
(28) Dahlberg, M. E., and Benkovic, S. J. (1991) Kinetic mechanism of DNA polymerase I (Klenow fragment): Identification of a second conformational change and evaluation of the internal equilibrium constant. *Biochemistry 30*, 4835−4843.
(29) Bloom, L. B., Otto, M. R., Beechem, J. M., and Goodman, M. F. (1993) Influence of 5′-nearest neighbors on the insertion kinetics of the fluorescent nucleotide analog 2-aminopurine by Klenow fragment. *Biochemistry 32*, 11247−11258.
(30) Garalde, D. R., Simon, C. A., Dahl, J. M., Wang, H., Akeson, M., and Lieberman, K. R. (2011) Distinct complexes of DNA polymerase I (Klenow fragment) for base and sugar discrimination during nucleotide substrate selection. *J. Biol. Chem. 286*, 14480−14492.
(31) Li, Y., and Waksman, G. (2001) Crystal structures of a ddATP-, ddTTP-, ddCTP, and ddGTP- trapped ternary complex of Klentaq1: Insights into nucleotide incorporation and selectivity. *Protein Sci. 10*, 1225−1233.
(32) Astatke, M., Grindley, N. D. F., and Joyce, C. M. (1998) How *E. coli* DNA polymerase I (Klenow fragment) distinguishes between deoxy- and dideoxynucleotides. *J. Mol. Biol. 278*, 147−165.
(33) Patel, P. H., Suzuki, M., Adman, E., Shinkai, A., and Loeb, L. A. (2001) Prokaryotic DNA polymerase I: Evolution, structure, and "base flipping" mechanism for nucleotide selection. *J. Mol. Biol. 308*, 823−837.
(34) Turner, R. M., Jr., Grindley, N. D. F., and Joyce, C. M. (2003) Interaction of DNA polymerase I (Klenow fragment) with the single-stranded template beyond the site of synthesis. *Biochemistry 42*, 2373−2385.
(35) Suzuki, M., Baskin, D., Hood, L., and Loeb, L. A. (1996) Random mutagenesis of *Thermus aquaticus* DNA polymerase I: Concordance of immutable sites in vivo with the crystal structure. *Proc. Natl. Acad. Sci. U.S.A. 93*, 9670−9675.
(36) Nick McElhinny, S. A., Kumar, D., Clark, A. B., Watt, D. L., Watts, B. E., Lundström, E. B., Johansson, E., Chabes, A., and Kunkel, T. A. (2010) Genome instability due to ribonucleotide incorporation into DNA. *Nat. Chem. Biol. 6*, 774−781.
(37) Bebenek, K., and Kunkel, T. A. (1995) Analyzing fidelity of DNA polymerases. *Methods Enzymol. 262*, 217−232.
(38) Kiefer, J. R., Mao, C., Braman, J. C., and Beese, L. S. (1998) Visualizing DNA replication in a catalytically active *Bacillus* DNA polymerase crystal. *Nature 391*, 304−307.
(39) Warren, J. J., Forsberg, L. J., and Beese, L. S. (2006) The structural basis for the mutagenicity of O^6-methyl-guanine lesions. *Proc. Natl. Acad. Sci. U.S.A. 103*, 19701−19706.